Potential Fuel Benefits of Optimized Continuous Climb Operations at Schiphol

J. Klapwijk

22 February 2018

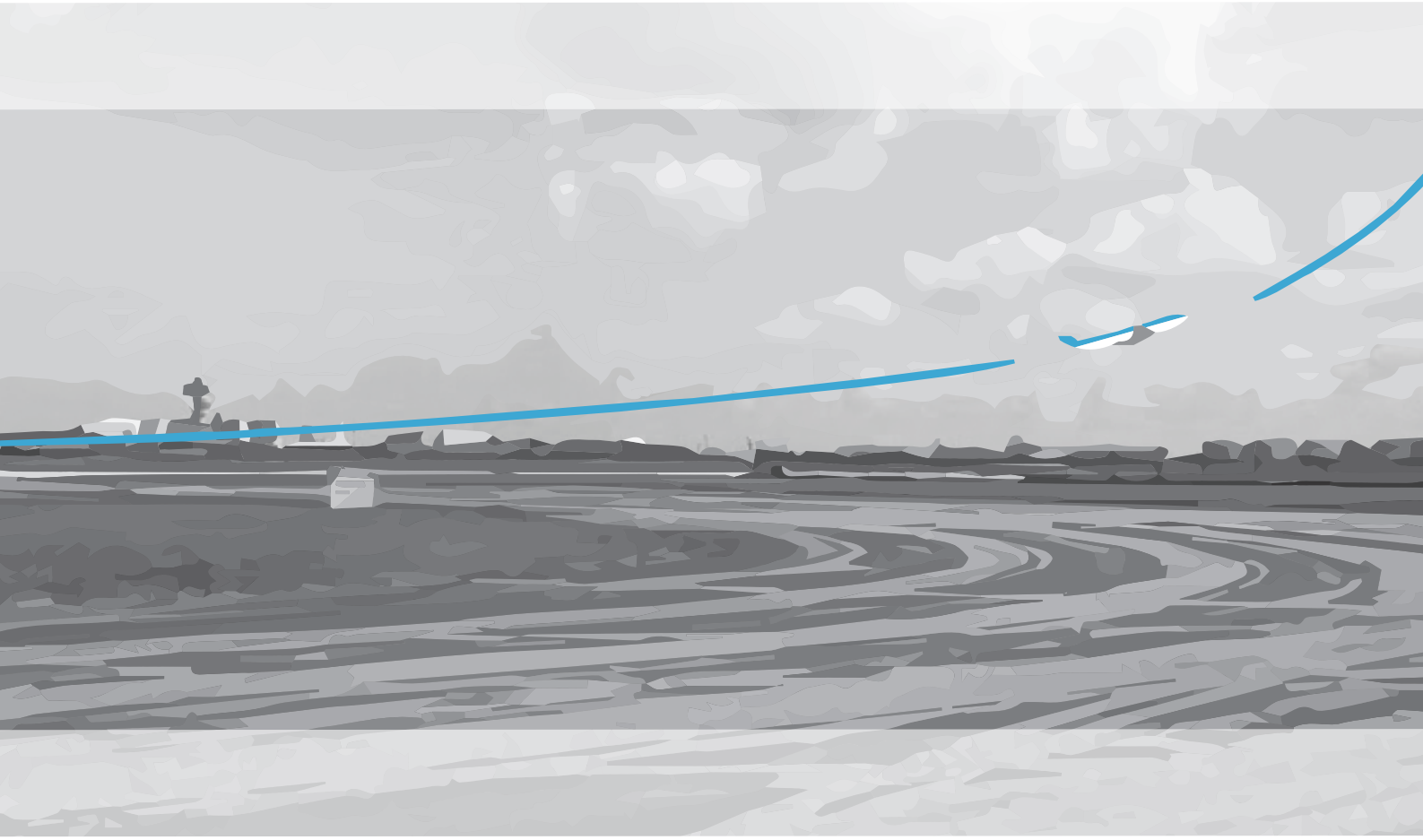

TU Delft Delft University of Technology

Challenge the future

Potential Fuel Benefits of Optimized Continuous Climb Operations at Schiphol

Thesis

Master of Science Thesis

For obtaining the degree of Master of Science in Aerospace Engineering
at Delft University of Technology

J. Klapwijk

22 February 2018

Faculty of Aerospace Engineering · Delft University of Technology

Delft University of Technology

Delft University Of Technology
Department Of
Control and Simulation

The undersigned hereby certify that they have read and recommend to the Faculty of Aerospace Engineering for acceptance a thesis entitled **"Potential Fuel Benefits of Optimized Continuous Climb Operations at Schiphol"** by **J. Klapwijk** in partial fulfillment of the requirements for the degree of **Master of Science**.

Dated: 22 February 2018

Readers:

dr.ir. J. Ellerbroek

Prof.dr.ir. J. M. Hoekstra

ir. P.C. Roling

C. Janssen (KLM)

Preface

By writing this preface I do not only finish my report, but also my final thesis and -after many years- my time as a student in Delft. A period in which my interests have grown, developed, scoped and refined. Finalizing this thesis feels like a rewarding end.

Regarding this thesis, I would like to thank my supervisors Jacco Hoekstra and Joost Ellerbroek for the guidance, support and valuable feedback. Furthermore, I would like to thank Ceriel Janssen for coaching me and offering a look behind the scenes at KLM. Finally I would like to thank Roberto Hofman for the numerous hours gathering data for my research.

Most important, I would like to thank my parents for their infinite support and my friends for making my time as a student unforgettable.

Jeffrey Klapwijk
Delft, 22 February 2018

Contents

List of Figures

List of Tables

Chapter 1

Report outline

This final thesis report consists of three individual parts. Part I contains a stand-alone scientific paper presenting the results of this study. Next, the appendices in part II extend the information presented in this paper with a level-off analysis, code flow diagrams and function explanations. Finally, part III contains the preliminary thesis report. This report has already been graded. Readers can refer to this document to learn more about the research proposal, data-sources and validation performed.

Part I

Scientific paper

Potential Fuel Benefits of Optimized Continuous Climb Operations at Schiphol

Jeffrey Klapwijk
Supervisors: Prof.dr.ir. Jacco M. Hoekstra, Dr.ir. Joost Ellerbroek
Control & Simulation, Department Control & Operations
Delft University of Technology, Delft, The Netherlands

***Abstract*—Continuous Climb Operations aim at improving the efficiency of a flight's climb phase by reducing the number of level-offs. The associated fuel-benefits help airlines and airports to comply with future emission demands, rising fuel prices and modernizing airspace requirements. Previously, most studies in this field only considered the effect of removing unintended level-off sections requested by Air Traffic Control (ATC). In this study, the effect of all current climb inefficiencies have been studied for Schiphol Airport in the Netherlands. By comparing historic radar tracks and on-board measured flight data with simulated optimized trajectories, potential fuel benefits have been calculated for three scenarios. It was found that on average, 39.9 kg of fuel could be saved per flight with minimum time loss compared to the original departure when abandoning the 250 knots speed restriction below FL100. As a result, 19.2 million kg fuel and 60.8 million kg CO_2 emissions could be reduced annually at Schiphol given the current traffic density.**

***Index Terms*—Continous Climb Operations, Optimized Climb, Fuel Benefits, Schiphol International Airport, KLM, Royal Dutch Airlines**

I. Introduction

In the last decade, research on flight efficiency became more relevant than ever due to increasing fuel-cost and emission regulations at airports. Besides improving the design of new aircraft, savings can also be achieved by optimizing current operations. In this category, Continuous Climb Operations (CCO) and Continuous Descent operations (CDO) are two promising initiatives. Because of the stair-step procedures followed by air traffic control, the regulations and the transition between airspace sectors, climb and descent phases of a flight are likely to contain horizontal segments (level-offs). These level-off sections are flown at sub-optimal speeds and altitudes and require more fuel than a comparable segment in the cruise phase.

Unfortunately, the number of studies performed on CCOs is limited. This is largely due to the fact that the frequency and duration of inefficiencies during landing is larger than during take-off [1]. Despite of this preference for descents, previous research on CCO does exist and has shown the potential to reduce fuel consumption ranging from 2 - 22 kg per flight [1]–[5]. The major drawback of these studies is that most only considered the removal of level-off segments. According to the CCO guidelines set by the International Civil Aviation Organization (ICAO), Continuous Climb Operations should facilitate a climb optimized for aircraft performance with a minimum number of constraints and regulations [6]. To better study the benefits of a continuous climb, new trajectories need to be simulated that fly according to the aircrafts optimum climb profile.

At Schiphol International Airport, current climb operations could be considered efficient. In the first half of 2017 less than 5% of all climbs experienced an unplanned level-off requested by ATC. However, due to speed restrictions and regulations aircraft are not allowed to fly optimum profiles. In light of this, the question arises how much current operations deviate from optimized Continuous Climb Operations. This paper investigates the potential annual fuel benefits if all flights at Schiphol would take-off using an operationally-optimal continuous climb profile compared to the current baseline operations. To fulfill this objective, the following three questions have been answered:

- What was the baseline annual fuel-consumption of all flights departing Schiphol in 2017?
- What is an operationally optimal climb profile?
- What is the estimated fuel consumption when all baseline flights climb optimal continuous climb profiles?

The hypothesis is that optimized continuous climb trajectories will on average save at least 20 kg of fuel per flight over current-day operations at Schiphol airport. This value is based on the largest average fuel-saving found by past research that only considered the removal of level-off sections [4].
The results of this study help to determine whether the benefits of CCO are sufficiently significant to justify a change of the current procedures at Schiphol. In a broader context, the objective of this research will be in line with international efforts such as SESAR and NextGen to deploy CCOs and CDOs in modern Air Traffic Management (ATM) solutions. This paper follows after a study performed by [7] on CDOs at Schiphol in 2016.

Section II will further outline the background of this research and provide the reader with an analysis of current operations. To answer the research questions, fuel-consumption for both historic and simulated CCO flights has been calculated. A general overview of this process is shown in Figure 1. Implementation and validation of the fuel-estimations model is explained in Section III. Next, Section IV explains how CCO

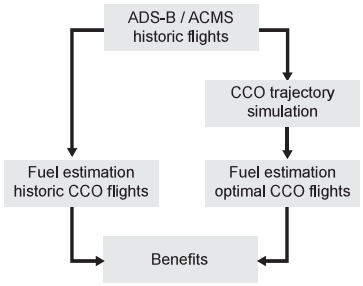

Fig. 1. Overview procedure followed to calculate CCO benefits

trajectories have been simulated for different scenarios. More details on these scenarios, data sources and the simulation design can be found in Section V. The results and annual benefits are presented in Section VI-VIII. These results are discussed in Section IX. Finally, recommendations for future research can be found in X. The paper ends with the conclusion in Section XI

II. Background

As mentioned in the introduction, more studies exist on CDOs than CCOs since the potential fuel-benefits of CDOs are larger. However, there are some practical differences that influence the implementation and feasibility of both continuous climb and descent operations. As a result, the benefits for CCO might be more realistic to achieve which emphasizes the relevance of research in this field.

A. Climb versus descent

Both CDOs and CCOs rely on flying a continuous path without interruptions. In current operations however, re-routing and vectoring of aircraft frequently occurs. Path shortening of a Continuous Descent Approach (CDA) could potentially lead to dangerous situations since the aircraft is descending at a much steeper path than a conventional descent. The opposite is true for CCOs, where path shortening could lead to reduced flight time, hence less fuel consumption. Path lengthening during a continuous climb eventually leads to a larger time spent at cruise altitude while path-extensions during a CDA require the aircraft to level-off or change flight path angle.

Furthermore, arriving aircraft in the terminal area are spaced and sequenced at strategic heights by ATC. When the airport demand peaks, airplanes are frequently placed in level holding patterns. This, together with the interception of the glide slope often requires level-offs during descent. A different strategy is used for take-off. Before departure, aircraft are spaced and sequenced on ground using separation standards. After take-off, planes diverge and accelerate. According to [3] this decompression effect is one of the reasons why todays operations are able to achieve near-continuous climb for most flights, as opposed to descent.

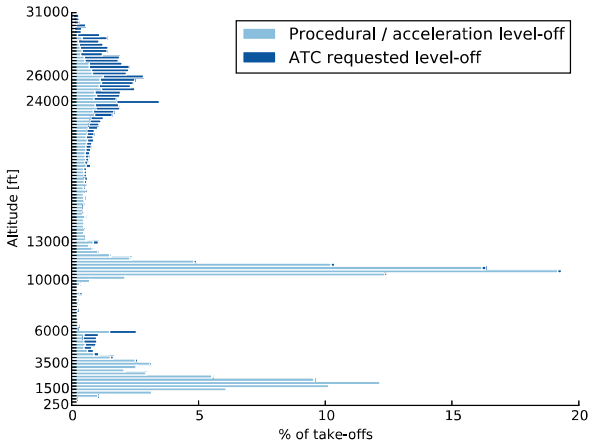

Fig. 2. Overview of level-off altitudes, types and the percentage of total flights that leveled-off at these altitudes. The two level-off types are stacked. One flight can level-off at multiple altitudes.

B. Identification of inefficiencies in current operations at Schiphol

Between take-off and cruising altitude, aircraft encounter one or more events which can lead to inefficiencies. A distinction was made between procedural level-offs (e.g. abatement procedures and speed restrictions) and supplemental ATC level-off requests. In general, level-offs of both categories can occur at each phase of the climb. The majority however clusters around key altitudes, as shown in Figure 2. Here, the horizontal axis shows the percentage of take-offs in 2017 that experienced a level-off at a certain altitude. The most frequent cause of level-offs is the speed limitation below 10000 feet. The main purpose of this restriction is to reduce the impact of bird-strikes and to better separate aircraft in the dense airspace around the airport. Above this altitude, aircraft are allowed to accelerate and most planes do this by slightly reducing the flight path angle. Some aircraft however, do this by leveling-off as can be seen in the figure. At 1500 feet, a similar situation occurs after the Noise Abatement Departure Procedure (NADP) when aircraft transition to their initial acceleration phase. Two other level-off altitudes at 6000 and 24000 feet are interesting since these are often imposed by ATC. The first one due to the interaction with inbound traffic streams at 7000 ft and the second due to upper-airspace transitions. Although these high-altitude inefficiencies occur more frequently, the low altitude ones have a larger impact on the fuel consumption [6]. The results of this analysis formed the basis of three different simulation scenarios described in Section V.

III. Fuel estimations using BADA 3.12

This study used the Base of Aircraft Data (BADA) 3.12 performance model by Eurocontrol [8] to estimate the fuel consumption of both historic flights as well as new optimized profiles. Based on altitude, airspeed, aerodynamic properties and thrust coefficients, fuel flow can be calculated. Although

the model has been validated for the climb phase of flight by independent studies [9], a validation has been performed in this paper to estimate the effect of assumptions and verify the implementation.

A. Equations and coefficients

The total fuel consumption is estimated by integrating fuel flow f_{nom} which is approximated using Eq. 1:

$$f_{nom} = C_{f1} \cdot \left(1 + \frac{V_{TAS}}{C_{f2}}\right) \cdot Thr \tag{1}$$

In this equation, V_{TAS} is True Airspeed (TAS) and the fuel-coefficients C_{f1} and C_{f2} are aircraft dependent parameters found in BADA's Aircraft Performance Operational File (OPF). The thrust Thr is calculated by rewriting the aircraft's longitudinal equation of motion. The result is a summation of kinetic and potential energy given by Eq. 2

$$(Thr - D) \cdot V_{TAS} = m \cdot g_0 \frac{dh}{dt} + m \cdot V_{TAS} \frac{dV_{TAS}}{dt} \tag{2}$$

With the height and speed known, the horizontal and vertical accelerations can be derived using a discrete differentiation method. For the Automatic Dependent Surveillance Broadcast (ADS-B) dataset, a reference mass from the OPF has been used since weight information is not present. The influence of this assumption can be seen in Table I. Also, the assumption was made that Ground Speed (GS) equals TAS due to the lack of wind-speed and wind-direction information in ADS-B transmissions. Here, the wind was assumed zero. The drag D can be calculated using Eq. 3

$$D = \frac{C_D \cdot \rho \cdot {V_{TAS}}^2 \cdot S}{2} \tag{3}$$

In this equation, true airspeed V_{TAS} and wing reference area S need to be provided. Air density ρ is dependent on altitude and can be calculated using the International Standard Atmosphere (ISA) model. The total drag coefficient can be obtained using the so-called drag polar in Eq. 4.

$$C_D = C_{D_0} + k \cdot C_L^2 \tag{4}$$

Parasite and induced drag coefficient C_{D_0} and k respectively, are aircraft specific and can also be found in the OPF. These values vary according to aircraft configuration and flight phase. BADA uses a 'clean' configuration for the climb phase. This corresponds to real-life operations where lift devices are retracted after the NADP. This study only considered the 2D vertical plane since lateral effects (routes) are outside the scope. Based on this, the bank angle is assumed to be zero in all calculations. The resulting lift coefficient can be calculated using Eq. 5.

$$C_L = \frac{2 \cdot m \cdot g_0}{\rho \cdot {V_{TAS}}^2 \cdot S} \tag{5}$$

B. Maximum climb thrust and minimum fuel flow

When estimating the fuel-flow based on horizontal and vertical acceleration, extreme values need to be capped to prevent unrealistic or even negative fuel flow estimations. To achieve this, minimum fuel flow and maximum thrust have been introduced. The latter value is also important for calculating new climb trajectories. If take-off weight allows for this, maximum reduced thrust is flown from NADP until cruise altitude, and the estimation of this value determines the excess power available for climb. The maximum available thrust is assumed to be independent of airspeed and dependent on altitude. Although the available thrust decreases with higher outside temperatures, this effect only starts to influence the engine performance coefficients above 26 $°C$. Considering Schiphol's geographic location and climate, it was assumed that a temperature correction factor was not required. The maximum thrust can therefore be approximated using Eq. 6.

$$Thr_{max} = C_{Tc,1}\left(1 - \frac{h}{C_{Tc,2}} + C_{Tc,3} \cdot h^2\right) \tag{6}$$

The minimum fuel-flow limit is given by:

$$f_{min} = C_{f3}\left(1 - \frac{h}{C_{f4}}\right) \tag{7}$$

The thrust coefficients $C_{Tc,1}$, $C_{Tc,2}$, $C_{Tc,3}$ and fuel-flow coefficients C_{f3}, C_{f4} can be found in BADA's OPF files. Furthermore, Eq. 6 and 7 are only valid for jet engines. Propeller and piston engines require alternative equations and have been neglected in this study.

The list below provides a summary of the assumptions stated in Section III:

- The bank angle is assumed to be zero.
- The equations and performance coefficients are valid assuming standard atmospheric conditions.
- Calculations assume zero temperature deviations compared to the ISA.
- Only aircraft with jet engines will be considered since these account for the majority of flight at Schiphol [10].
- Aircraft reference mass m_{ref} was used in combination with ADS-B data, since actual mass m_{act} was not available.
- Ground-speed V_{GS} was used in combination with ADS-B data, since V_{TAS} is not available.

C. Validation

Due to the availability of measured fuel flow in the Aircraft Condition Monitoring System (ACMS) data, validation and verification could be performed. Table I shows the result of this validation for the 9 aircraft types operated by KLM Royal Dutch Airlines (KLM). Each column represents the relative error between the estimated and measured fuel consumption for a particular assumption (e.g. reference mass or ground speed). The third and fifth column show the average error when using ACMS or ADS-B records respectively. The bottom-row gives the total weighted average error per assumption. This value is important since it gives an indication of how much the total

TABLE I
EFFECT OF ASSUMPTIONS ON AVERAGE FUEL ESTIMATION ERROR [%] OF BADA 3.12 PERFORMANCE MODEL DURING CLIMB PHASE AT SCHIPHOL

AC model	count	V_{TAS} m_{act} error [%]	V_{GS} m_{act} error [%]	V_{GS} m_{ref} error [%]
A332	171	-1.7	-0.3	-6.5
A333	140	0.4	0.3	-12.6
B737	1295	4.2	7.3	8.3
B738	1675	0.7	3.0	2.0
B739	323	-4.0	-1.5	1.7
B744	222	-4.1	-2.2	-16.5
B772	379	-4.2	0.9	-18.9
B77W	218	-3.6	1.6	-12.7
B789	396	-0.7	0.4	-10.8
Weighted average [%]	**4819**	**0.30**	**2.97**	**-1.25**

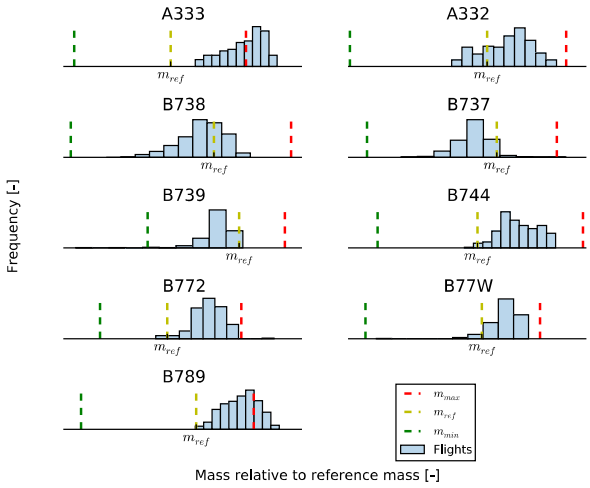

Fig. 3. Historic take-off weight distribution for KLM aircraft departing Schiphol. BADA's minimum, reference and maximum take-off weight are indicated with vertical dashed lines. KLM operates different versions of the A333 and B789 with an extended maximum take-off weight compared to the models used in BADA, explaining the distributions exceeding m_{max}.

extrapolated end-result in Section VIII differs from reality. It is clearly visible that the reference mass (m_{ref}) assumption has the largest influence on the error, especially for long-range heavy-weight aircraft (A333, B744, B772/W and B789). This error can be explained when comparing KLM's historic take-off mass distribution (from the available ACMS records) with the reference mass in Figure 3. Furthermore, the Boeing 737-700 is one of the most frequently occurring aircraft in this dataset and the large estimation error of 7.3% (fourth column) when using GS instead of TAS significantly influences the total weighted average.

IV. CLIMB TRAJECTORY MODELS

Past research has shown that climbing close to maximum climb rate approximates a minimum fuel climb [11] [12]. The idea behind this is that air-density and therefore drag decreases with altitude. To reduce fuel, the time in the dense low-altitude air needs to be minimized by climbing as fast as possible. This approximation is valid when assuming that engine thrust is constant with airspeed and the available thrust decreases linear with altitude. In reality, true optimization of a climb with multiple objectives (cruise altitude, speed, initial acceleration) requires the use of more complex algorithms (e.g. genetic algorithm or calculus of variations) to determine [13]. Climbs that result from this optimization have an unrealistic profile for current civil operations. Furthermore, the computational effort required to do this would have been too large to simulate the number of flights in this study. As a result, the flights in this study are optimized on maximum rate-of-climb (or minimum time-to-climb), with the above mention assumptions.

Under normal circumstances and if the take-off weight allows for this, planes are climbing with maximum reduced thrust until cruising altitude. With this knowledge, the only unknown variable is the airspeed at which the plane has to climb. The flown airspeed directly influences the amount of excess power left to climb, hence the rate-of-climb.

Based on three scenarios that will be explained in Section V-C, two separate trajectory models have been constructed. A sketch of a single time step in both models given in Figure 4. Starting at t_i, the next ($\Delta t = 1s$) time step t_{i+1} can be calculated using:

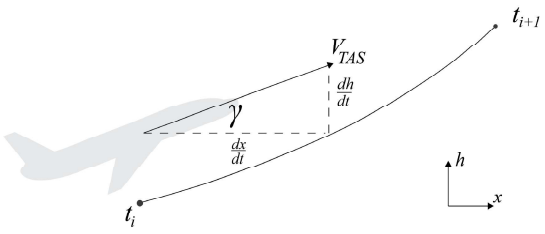

Fig. 4. Sketch of a time-step in the trajectory model

$$h(t_{i+1}) = h(t_i) + \frac{dh}{dt}$$
$$V_{TAS}(t_{i+1}) = V_{TAS}(t_i) + \frac{dV_{TAS}}{dt}$$
$$x(t_{i+1}) = x(t_i) + \frac{dx}{dt}$$

With starting conditions known, these equations can be solved by isolating $\frac{dh}{dt}$, $\frac{dv}{dt}$, $\frac{dx}{dt}$ from Eq. 2:

$$\frac{dh}{dt} = \frac{(Thr - D)V_{TAS}}{m \cdot g_0} \cdot C_{red} \cdot f\{M\} \tag{8}$$

$$\frac{dv}{dt} = \frac{dv}{dh}\frac{dh}{dt} = \left[\left(\frac{1}{f\{M\}} - 1\right)\frac{g_0}{V_{TAS}}\right]\frac{dh}{dt} \tag{9}$$

$$\frac{dx}{dt} = \sqrt{V_{TAS}^2 - \left(\frac{dh}{dt}\right)^2} \tag{10}$$

The reduced thrust coefficient C_{red} of jet engines can be approximated as a function of actual, minimum and reference

mass. The coefficient increases to 1 if the actual mass approaches the maximum take-off mass, hence full thrust will be applied.

$$C_{red} = 1 - 0.15 \cdot \frac{m_{max} - m_{act}}{m_{max} - m_{min}} \tag{11}$$

Furthermore, $f\{M\}$ represents the Energy Share Factor (ESF) as introduced in BADA [8]. This factor can be substituted with the original term found when rewriting Eq.2.

$$f\{M\} = \frac{1}{1 + \frac{V_{TAS}}{g_0}\frac{dV_{TAS}}{dh}} \tag{12}$$

In this study, the method to calculate $f\{M\}$ depends on the type of climb: optimized constant Calibrated Airspeed (CAS) or optimized TAS. A detailed explanation is given in the following two subsections. The third subsection explains the framework around these two models. Finally, the last subsection illustrates the mass sensitivity of climb trajectories and the implications of this.

A. Model 1: optimized constant CAS climb

In most commercial aircraft, the Flight Management System (FMS) can provide an optimum airspeed that will achieve the desired time and cost requirements for a given Cost Index (CI). There exists a certain constant CAS airspeed which results in a CI of 0 [14]. In other words: a climb in which fuel is infinitively more important than time. Finding this airspeed in our simulation will result in a fuel-optimized and operationally-feasible climb trajectory.

Based on this, model 1 generates a trajectory that maintains a constant CAS throughout the climb until the Mach / CAS transition. To maintain the required CAS, the TAS needs to increase so a portion of the excess power is used to accelerate. This allocation of power is calculated using the ESF equations given by Eq. 13-16. Here, γ represents the ratio of specific heats c_v and c_p, instead of the flight path angle. The remaining power is used to climb. Initially, the aircraft accelerates to the pre-defined CAS setting using $f\{M\} = 0.3$. This value corresponds to nominal acceleration of commercial aircraft [8]. When achieving the desired airspeed, the aircraft climbs according to:

$$f\{M\} = \left[1 + \frac{\gamma R\beta}{2g_0}M^2 + \left(1 + \frac{\gamma-1}{2}M^2\right)^{\frac{-1}{\gamma-1}}\left(\left(1 + \frac{\gamma-1}{2}M^2\right)^{\frac{\gamma}{\gamma-1}} - 1\right)\right]^{-1} \tag{13}$$

Above the tropopause, the equation reduces to:

$$f\{M\} = \left[\left(1 + \frac{\gamma-1}{2}M^2\right)^{\frac{-1}{\gamma-1}}\left(\left(1 + \frac{\gamma-1}{2}M^2\right)^{\frac{\gamma}{\gamma-1}} - 1\right)\right]^{-1} \tag{14}$$

When the Mach/CAS transition takes place below the tropopause, the aircraft will continue climbing at constant Mach number which reduces the ESF further to:

$$f\{M\} = \left[1 + \frac{\gamma-1}{2}M^2\right]^{-1} \tag{15}$$

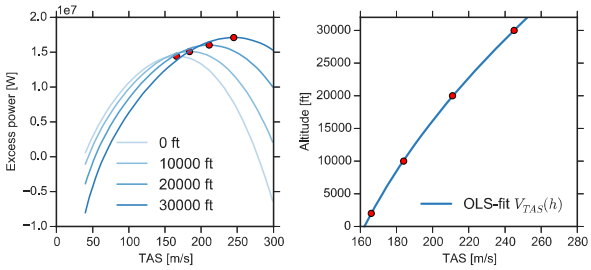

Fig. 5. Excess power curves for various altitudes with corresponding second order fit $V_{TAS}(h)$ for B738 (m_{ref})

Flying at constant Mach above the tropopause requires no deceleration or acceleration. In other words, all the excess power can be used to climb:

$$f\{M\} = 1 \tag{16}$$

B. Model 2: optimized TAS climb

For each combination of mass and altitude, a true-airspeed exists at which the difference between power available and power required is largest. In other words, where the climb rate is largest. As can be seen in Figure 5, this airspeeds changes with altitude and the corresponding relation $v(h)$ was found numerically by fitting a second-order ordinary least squares function through the peaks of the excess power curves P_e. These curves can be calculated using Eq. 17 for a range of densities.

$$P_e = Thr_{max}V_{TAS} - \frac{C_D \cdot \rho \cdot {V_{TAS}}^3 \cdot S}{2} \tag{17}$$

The resulting least squares fit has the form:

$$V_{TAS}(h) = a_0 + a_1 h + a_2 h^2 \tag{18}$$

In this function, a_0 is the initial acceleration speed. Coefficients a_1 and a_2 are used in the altitude derivative:

$$\frac{dV_{TAS}}{dh} = a_1 + a_2 h \tag{19}$$

To calculate the ESF, Eq. 19 has been substituted in Eq. 12. Although the a_0 value found corresponds to the theoretical airspeed at which the rate of climb is maximized, it was found that this does not always result in the most fuel-economical climb. When the desired cruising altitude and cruising Mach number are low, it is not always best to accelerate to the optimum airspeed. Furthermore, the curves in Figure 5 show that a 10 to 20 m/s offset from the absolute maximum nearly yields the same excess power as the maximum itself. To find an optimum that also takes cruising altitude, cruise Mach and initial acceleration into account, the simulations have been iterated for various offset values of a_0. In other words, the initial airspeed was varied while maintaining the same $\frac{dv}{dh}$ ratio (a_1, a_2).

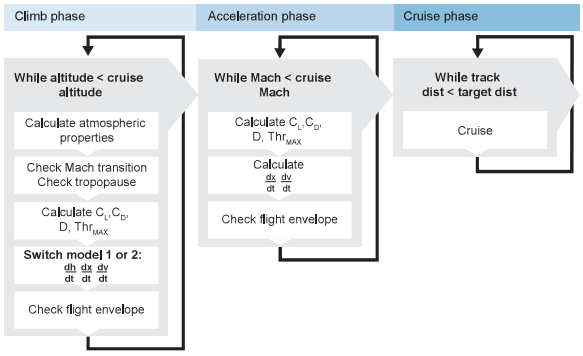

Fig. 6. Flowchart of the framework around climb model 1 and 2

C. Model framework

A flowchart of the structure around models 1 and 2 can be seen in Figure 6. The general principle is to start at a given altitude, speed and distance: h_0, v_0 & x_0 with a desired cruising altitude and target Mach number. These values are used to calculate the atmospheric properties. Next, the aerodynamic properties and maximum reduced thrust are calculated. Depending on model 1 or 2, the new state derivatives will be updated. This loop continues until the cruise height has been reached. From this point on, all excess energy will be used to accelerate to the pre-determined speed and distance. The latter is necessary to ensure a fair comparison between the different profiles. An aircraft with a higher constant CAS/ Mach setting will have traveled a longer distance when reaching cruise altitude than one climbing at a lower speed. The entire process is repeated for a range of CAS values (model 1) or a range of a_0 values (model 2). An example of the output can be seen in Figure 8.

D. Mass sensitivity

Without knowing the accurate take-off mass, fuel-benefit calculations can become unreliable. It was found that the mass has a larger effect on the climb profile than the airspeed. In other words, if the mass of the simulated aircraft was estimated lower than the actual flown mass, the climb profile would reach the cruise phase minutes before the original flight and the resulting fuel savings would be due to a lower mass and not an optimized trajectory.

To illustrate this, the fuel consumption of a historic A330-300 flight from the ACMS dataset is shown in Table II. Since we know the actual mass, the fuel calculations are reliable and estimated to be 5880 kg. Next, the flight trajectory is optimized using scenario 2, reducing the fuel consumption to 5813 kg (-87 kg) and shortening the climb duration with 22 seconds.

The second row in Table II illustrates the situation when a reference mass has been used as done with ADS-B data. As expected, the fuel calculation of the same historic profile turns out lower (5428 kg) due to the lower mass. The climb duration remains the same since the historic trajectory is unchanged. The new trajectory however has been optimized for the reference weight and follows a completely different

TABLE II
INFLUENCE OF MASS ACCURACY FOR A330-300

		Historic climb		**Simulated CCO**	
	Mass [kg]	Fuel [kg]	t [s]	Fuel [kg]	t [s]
m_{act}	198927	5880	2248	5813	2226
m_{ref}	174000	5428	2248	5281	2272

climb profile. The newly simulated profile reaches the cruise altitude faster at a lower speed and then spends relatively more time in the cruise phase. The original flight was heavier, required more airspeed and spent more time in the dense air. As a result, the comparison between the two is unfair. The resulting savings (147 kg) are due to the lower mass and not due to the actual optimization.

Since in most cases the take-off weight is not normally distributed around the m_{ref} (Figure 3), batch simulations will result in either positive or negative estimates of the annual fuel consumption. As a result of this, aircraft types that were only covered by the ADS-B data have been calculated for various weight assumptions.

V. SIMULATION DESIGN

This section will explain the batch simulations process performed in this study. First, an overview will be given of the simulation structure. This structure consists of the trajectory framework and the BADA performance model. Next, the two data sources (ACMS and ADS-B) which form the input of the simulation are discussed. The section continues by introducing 3 scenarios that are based in the inefficiencies found in Section II. Finally, the outputs of the simulation are explained.

A. Overview batch simulation process

The data of a single historic flight runs along 4 different paths as shown in Figure 7. The first path calculates the original fuel consumption. The other paths run through the different optimization scenarios. Each scenario copies and uses the first 1500 ft from the historic flight and retrieves the original cruising altitude, cruise speed a range of pre-defined CAS speeds that will be simulated. Afterwards, the fuel consumption of all simulated CCO trajectories is calculated and compared with the original baseline flight. For each scenario, the most optimal climb is stored.

B. Simulation input: data sources

Two sources of flight data were available for this study. The majority of flights has been covered by ADS-B data which contains only basic information such as location, altitude and ground-speed. A part of these flights will have additional ACMS data provided by KLM. The benefit of this source is the availability of additional information such as weather, mass, Indicated Airspeed (IAS) and TAS. Table VI provides an overview of take-offs in 2016 based on Schiphol's annual traffic review [10]. Since the 2017 review was not yet available during this study, an estimate of the traffic was made based on both data-sources. The last two columns in Table VI show the number of used records for this study.

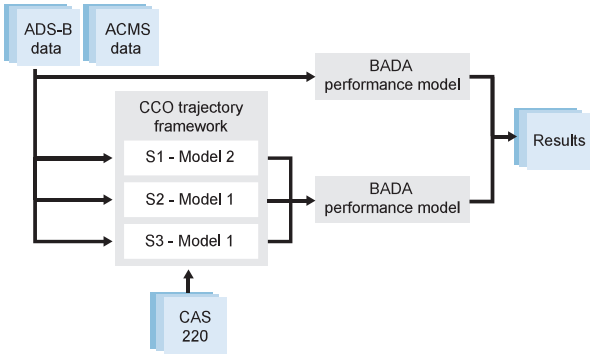

Fig. 7. Overview of batch simulation process.

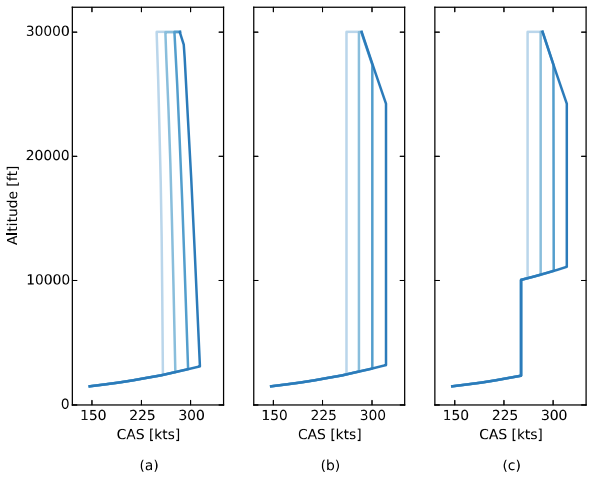

Fig. 8. Example (B737, m_{ref}, $M_{cruise} = 0.7$) of speed-altitude profiles generated for scenario 1 (a), 2 (b) and 3 (c). Scenario 2 and 3 use climb model 1. Scenario 1 uses climb-model 2. Different lines illustrate the various CAS values tried.

C. Scenarios

Three scenarios were chosen based on the inefficiencies found in Section II. All scenarios have in common that they start the optimization at 1500 ft, right after the NADP 2. Furthermore, they all fly a constant Mach climb after the Mach-transition. This Mach number is similar to the cruise Mach of the original flight. An example of the simulation output for the various scenarios is given in Figure 8.

1) Scenario 1: Optimized TAS climb without restrictions using model 2. This concept provides insight in how much the operationally feasible profiles in scenario 2 and 3 differ from a theoretical optimum and if this difference is significant and worth developing new technologies.

2) Scenario 2: Optimized constant CAS climb without speed restriction below FL100 using model 1. This concept provides insight in how much fuel can be saved without the speed restriction while still flying according to current constant CAS procedure.

3) Scenario 3: Optimized constant CAS climb including the speed restriction below FL100 using an adapted version of model 1. This concept lies closest to current operations and assesses the influence of ATC induced level-offs. In other words, the new flight tries to mimic the historic flight and evaluates the difference in time and fuel consumption if aircraft would fly fuel-optimized profiles (CI = 0) with current regulations and restrictions.

D. Simulation output: dependent variables

The output of the simulations are the dependent variables: fuel benefits, climb duration difference and optimal airspeed. Obviously, the fuel benefits have been the main emphasis of this paper. Flight time difference is a good measure to investigate the feasibility of CCO implementation. Finally, the airspeed has been used to investigate how much the optimum speed deviates from current operations.

VI. Results ACMS data

As shown in Section III and IV, ACMS data provides the most reliable results due to the availability of mass and TAS data. A specification of the number of analyzed ACMS flights can be found in Table VI. Results with a time difference larger than 10000 s or a fuel reduction difference of $\pm$ 1000 kg have been ignored since these are a result of an extremely longer or shorter simulated climb. In the majority of the cases, this was due to an on-board measurement error of the initial fuel quantity. As a result, the simulated aircraft was not able to obtain its required cruising altitude or reached the altitude too fast. Other reasons that occur are incorrect estimation of the original cruising altitude or cruising speed since these values are calculated as the average of the last 5 measured seconds of a flight record.

A. Fuel benefits

The fuel benefits for the three scenarios are shown in Figure 9. It makes sense that the heaviest aircraft types have the largest saving potential since these consume more fuel per second. For all aircraft types, the third scenario has the lowest estimated fuel reduction. This result is expected since scenario S3 has the largest similarity with the original flight. Furthermore, the lightest aircraft types (B737, B738 and B739) show the least difference between the scenarios. This can be explained by the fact that their optimal speed is closer to the 250 kts. speed limit than for example a B777. Removal of this speed limit (as done in S2 and S3) does not result in a large difference compared to the current situation.

It can be seen that for most aircraft types, the data is slightly skewed and not always normally distributed. This is a plausible result since the amount of fuel that can be saved is, among other reasons, largely dependent on the take-off mass which is not normally distributed as can be seen in Figure 3. The fact that the data is skewed also

results in quite a few outliers next to the right whisker. However, most of these records are valid and show the cases where the original flight was relatively inefficient due to for example an ATC requested level-off. For this reason, the averages including outliers have been used in Section VIII.

Finally, it can be seen that the B744, B772 and B789 simulations in scenario 3 perform worse than the original flight. Figure 10 shows the average on-board measured IAS in the speed restricted altitude range. It was found that these aircraft types generally violate the speed restriction by requesting a high speed departure. As a result, the simulation flew slower than the original flight hence, consumed more fuel. Although these aircraft generally exceed the maximum take-off speed, they still fly 50 to 70 knots below their optimum speed shown in Figure 12.

Considering take-off mass and optimum airspeed, the B789 can be positioned in a similar category as the A332 and A333. Unlike the A332 and A333, the B789 frequently climbs with a speed higher than the maximum take-off speed as seen in Figure 10. As a result, the B789 often flies closer to its optimum speed than the A332 and A333. This is one possible explanation why the estimated fuel savings of the B789 are significantly lower than the comparable airbus models for all scenarios.

Visually, the first two scenarios outperform the third scenario and there is no large difference between the first and second. To investigate if the optimized TAS climb (S1) is significantly better than the optimized CAS climb (S2), statistical tests have been performed. Since all aircraft fly all scenarios and there is only one independent variable (the scenario type) with more than one category, Friedman's ANOVA test was used. The various dependent variables (fuel benefits, optimal airspeed, flight duration) have been tested separately. Due to the large number of samples for each one of the aircraft types, even the small difference found between the scenarios are often proven significant. Based on this, the distinction has been made between significant ($p < 0.01$) and marginally significant ($p < 0.05$). The pairwise comparisons have been adjusted by the Bonferroni correction. It was found that for all aircraft types the small differences in fuel reduction between the scenarios is significant (Table III). This proves that, even though S1 and S2 seem visually similar and the variation of airspeed in S1 approximates a constant CAS climb, flying an actual constant CAS climb does result in losses compared to a non-constant CAS climb.

B. Climb duration difference

Figure 11 shows that on average, all of the simulated flights differ less than $\pm$ 150 seconds with respect to the original flight and most aircraft stay within $\pm$ 60 seconds difference. Intuitively, climbing according to a maximum climb rate would result in a longer flight time since altitude has priority over distance. However, the optimal speed below 10000 ft of the B744, B772 and B77W differs so much from

TABLE III
RELATED SAMPLES FRIEDMAN'S ANOVA TEST. REJECTING THE NULL HYPOTHESIS THAT THE FUEL SAVINGS BETWEEN THE 3 SCENARIOS ARE THE SAME WITH INDICATED SIGNIFICANCE

AC	Significance
A332	$\chi^2(2) = 1.49 \cdot 10^3, p < 0.01$
A333	$\chi^2(2) = 1.49 \cdot 10^3, p < 0.01$
B77W	$\chi^2(2) = 1.25 \cdot 10^3, p < 0.01$
B737	$\chi^2(2) = 5.91 \cdot 10^3, p < 0.01$
B738	$\chi^2(2) = 1.30 \cdot 10^4, p < 0.01$
B739	$\chi^2(2) = 0.32 \cdot 10^3, p < 0.01$
B744	$\chi^2(2) = 1.38 \cdot 10^3, p < 0.01$
B772	$\chi^2(2) = 2.80 \cdot 10^3, p < 0.01$
B789	$\chi^2(2) = 0.16 \cdot 10^3, p < 0.01$

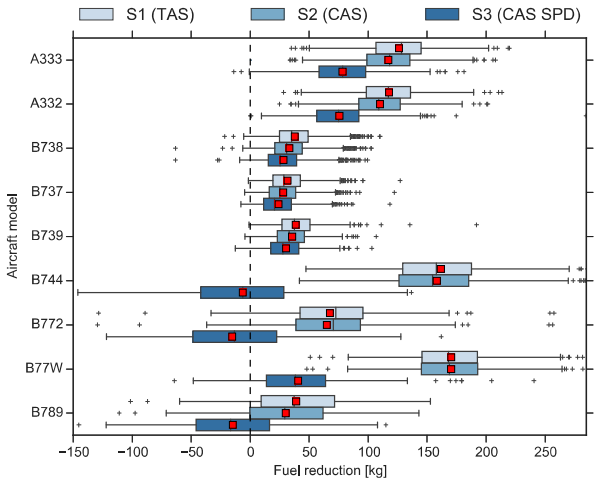

Fig. 9. Estimated fuel-benefits for 3 scenarios using ACMS data. The red square visualizes the average including outliers

the current speed limit that these aircraft can compensate the extra time required to fly at maximum climb rate with the increased airspeed they fly during the climb. This results in a positive flight-time reduction. The majority of outliers can be found next to the right whisker, similar to what can be seen with the fuel benefits in Figure 9. These outliers represent extreme flight time reduction due to inefficient baseline flights.

Comparing the concepts, it was found that for most aircraft types there is no significant difference in climb duration between S1 and S2 for A332 ($p > 0.05$), A333 ($p > 0.05$), B737 ($p = 0.022$), B738 ($p = 0.041$), B738 ($p > 0.05$), B744

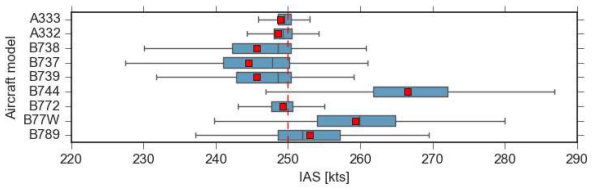

Fig. 10. Measured IAS between 3000ft and 9500 ft of KLM ACMS records

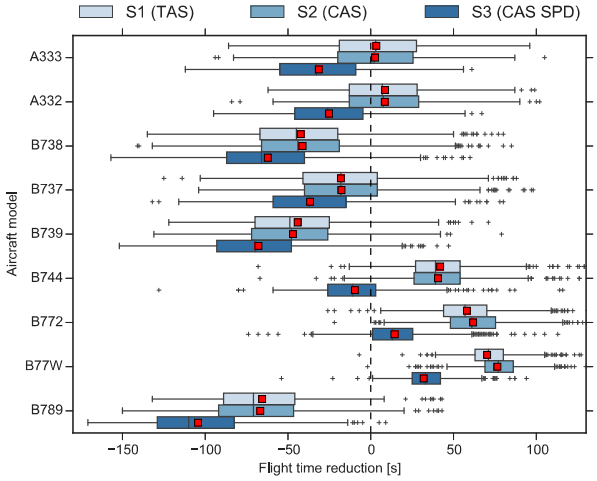

Fig. 11. Flight time difference compared to original profile for 3 scenarios using ACMS data. The red square visualizes the average including outliers

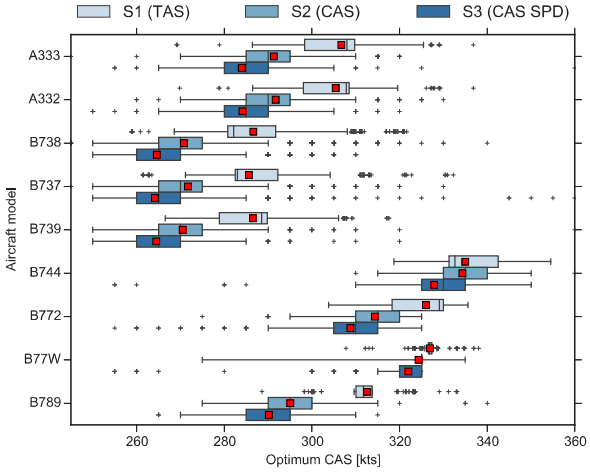

Fig. 12. Optimum constant CAS airspeed for 3 scenarios using ACMS data. For scenario S1, the values should be interpreted as initial acceleration speeds. The red square visualizes the average including outliers.

$(p = 0.015)$ and B789 $(p > 0.05)$.

C. Optimal airspeed

The optimal climb-speed depends on aircraft type, mass, target speed and altitude. As a result, each aircraft model has a range of optimal airspeeds shown in Figure 12. For scenario 1, the CAS values shown are the target airspeed right after NADP at 1500 ft. In other words, the value of a_0 in Eq. 18. Although not visible in Figure 12, the CAS of scenario 1 decreases approximately 10-15 kts throughout the climb. For scenarios 2, the CAS values represent the constant CAS flown between 1500 ft and the Mach/CAS transition. Scenario 3 starts the optimization after the speed restriction. The values shown are therefore the constant CAS values between 10000 ft and the Mach/CAS transition.

It is clearly visible that for all aircraft types the initial optimal speed after take-off is largest in scenario 1. The difference in speed between scenario 2 and 3 can be explained by the fact that in scenario 3, the first 10000 ft are already flown at 250 kts before optimization can start. Above this altitude the optimum speed is already lower compared to the optimum speed at 1500 ft so the trajectory model will find a lower ideal airspeed.

Finally, aircraft with a larger take-off mass have a higher optimal airspeed and the difference in speed between flying S2 or S1 decreases.

VII. Results ADS-B data

Due to the lack off mass information and the large size of the dataset, ADS-B simulations have been performed only for scenario 2. This scenario lies closest to the ICAO definition of a CCO [6] and has the highest potential benefits while still being operationally feasible. All the simulations have been performed multiple times for the mass estimates: m_{min}, m_{ref} and m_{max}. The resulting fuel benefits, climb duration difference and optimal airspeed are given in Figure 13, 14 and 15 respectively. In these figures, only the result for aircraft types not included in the ACMS data are shown. Based on Figure 3 it is expected that the majority of flights has a take-off mass between m_{ref} and m_{max}. To further scope the information presented in this paper, only these results are shown.

The large number of outliers in both reference and maximum mass scenario are an indication that most flights fly with a different mass than assumed in the simulations. Also, the m_{max} scenario in Figure 13 shows a larger spread of data with mostly negative average fuel-benefits compared to the m_{ref}. This means that on average, the original flight was always more efficient than the newly simulated flight. From this it can be concluded that aircraft with a more negative average saving have been flying closer to m_{ref} than m_{max} and the other way around.

In general, the ADS-B results are similar to the ACMS results in terms of observations. However, the F70 is the only aircraft with an optimal speed lower than the 250 knots speed restriction. It can be seen in Figure 15 that the range of CAS values tried was insufficiently low to accurately investigate this aircraft. As a result, the fuel savings found for this model can be considered conservative. Since all F70s have been replaced in 2017, other aircraft types such as the E190/5 and E170/5 are expected to fill this gap in 2018. These new aircraft types benefit more from flying optimized CCOs as can be seen in Table VII.

VIII. Annual benefits

Table VI shows the 20 aircraft types that most frequently departed at Schiphol in 2017. The numbers are conservative since parts of December and October are missing in the

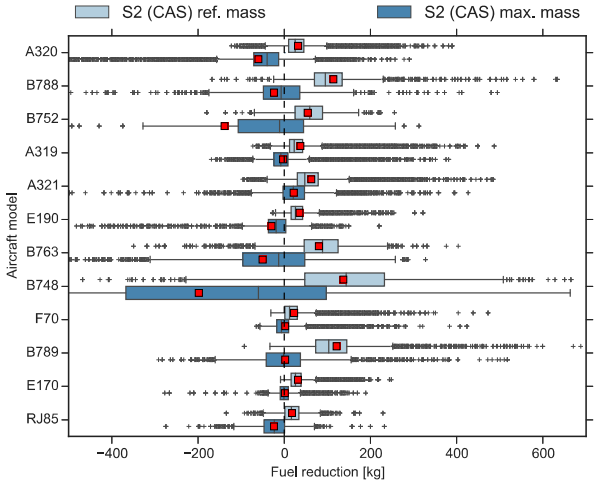

Fig. 13. Estimated fuel-benefits for scenario 2 using both reference and maximum take-off weight (ADS-B data). The red square visualizes the average including outliers

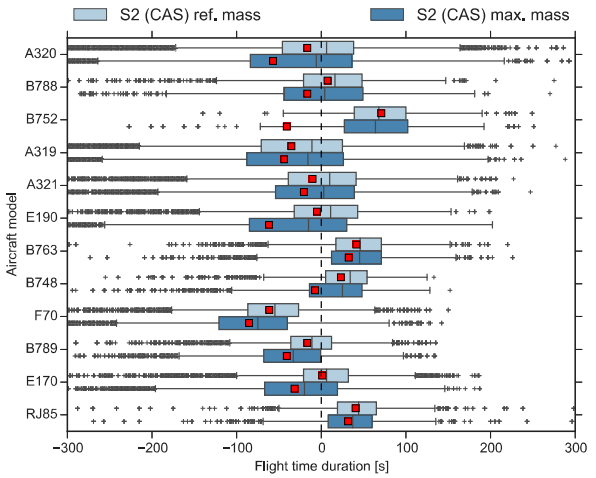

Fig. 14. Climb duration difference compared to original flight for scenario 2 using ADS-B data. The red square visualizes the average including outliers

dataset. As a result, the actual number of departures and total fuel savings will be higher. To calculate the annual benefits, the average saving per aircraft type (Table IV and VII) have been multiplied with the corresponding number of take-offs in Table VI.

The average fuel consumption found with the ADS-B data is not completely accurate as explained before. Interestingly, 58.3% of all annual take-offs can be covered by only considering aircraft types occurring in the ACMS data (Table VI). These fuel savings can be seen in Table V. The difference between scenario 1 and 2 is 1 million kg per year, which is 8.2% of the maximum achievable theoretical savings. The difference between scenario 2 and 3 is 5.2 million kg. This

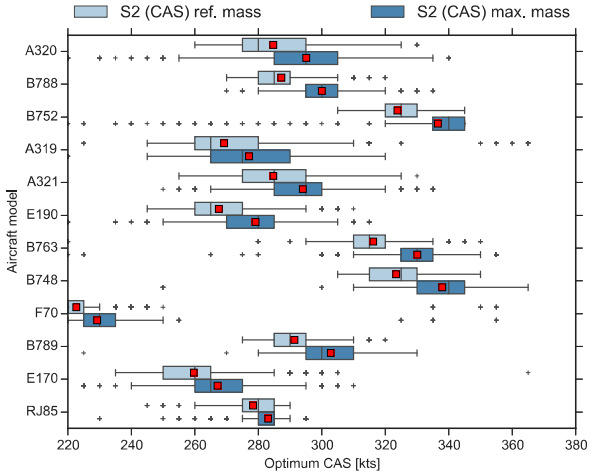

Fig. 15. Optimum CAS airspeed for scenario 2 using ADS-B data. The red square visualizes the average including outliers

TABLE IV
OVERVIEW OF AVERAGE FUEL SAVINGS PER FLIGHT FOR ALL THREE SCENARIOS FOR ACMS ANALYZED MODELS

	S1 [kg]	**S2** [kg]	**S3** [kg]
A332	118.3	110.6	75.8
A333	126.2	117.2	78.6
B737	31.7	28.0	24.0
B738	38.2	33.6	28.7
B739	58.2	45.4	39.5
B744	161.7	158.2	-6.6
B772	67.5	65.0	-15.2
B77W	170.9	170.4	40.4
B789	33.6	24.7	-20.0

entire difference is caused by the speed limitation below 10000 feet.

For the remaining models that are only found in the ADS-B dataset, it can be stated that there is a maximum saving potential. This potential can only be achieved when all aircraft take-off with a reference mass. In reality, this is not the case so the average savings will turn out between zero and maximum potential. The potential annual savings of the ADS-B dataset is shown in Table VII and have been estimated up to 8 million kg. When combining both ACMS and ADS-B predictions for S2, a saving-potential of 19.2 million kg fuel could be achieved, resulting in a reduction of 60.8 million kg CO_2 emissions each year [15].

IX. DISCUSSION

The fuel benefits found in scenario 1 and 2 require the aircraft to accelerate to an airspeed higher than currently done at an altitude of 1500 ft. This means that a larger area around Schiphol will be affected by noise. On the other hand, since aircraft are climbing at a faster rate, they also leave the dense Terminal Manoeuvering Area (TMA) around the airport faster.

TABLE V
PREDICTED ANNUAL SAVINGS FOR ALL THREE SCENARIOS FOR ACMS ANALYZED AC MODELS

	S1 10^5 kg	**S2** 10^5 kg	**S3** 10^5 kg
A332	11.1	10.4	7.1
A333	15.4	14.3	9.6
B737	13.3	11.8	10.1
B738	38.1	33.6	28.6
B739	5.9	4.6	4.0
B744	16.6	16.2	-0.7
B772	6.7	6.4	-1.5
B77W	13.7	13.7	3.2
B789	1.1	0.8	-0.7
Annual savings	122.0	111.8	59.8

TABLE VI
NUMBER OF ANALYZED ADS-B AND ACMS FLIGHTS FROM 2017 COMPARED WITH THE NUMBER OF DEPARTURES IN 2016

	2016	2017	2017
	Traffic review [10]	**Analyzed ADS-B flights**	**Analyzed ACMS flights**
B738	99821	130135	6602
A320	51676	67545	
B737	42010	52186	5138
A319	34209	46233	
F70	29306	19184	
A321	11975	18226	
E170/5	11094	17232	
B744	16197	16845	765
A333	12238	16131	526
B772/L	16164	21102	1512
B773/W	8016	13171	876
B739	10209	12436	1325
A332	9421	12117	799
E190/5	72180	10587	
B763	5611	6557	
B789	3419	6432	394
RJ85	5112	5774	
B788	3313	3810	
B748	2306	2929	
B752	2346	2667	
Total	446623	481299	17937

TABLE VII
OVERVIEW OF AVERAGE FUEL SAVINGS (S2) FOR REMAINING MODELS ONLY COVERED BY ADS-B DATA. THE VALUES SHOWN ARE ASSUMMING REFERENCE MASS

		Average saving	**Annual potential**
	#	kg	10^5 kg
A320	67545	32.1	21.7
A319	46233	37.5	17.3
F70	19184	22.8	4.4
A321	18226	63.1	11.5
E170/5	17232	32.1	5.5
E190/5	10587	35.6	3.8
B763	6557	80.5	5.3
RJ85	5774	18.1	1.0
B788	3810	114.0	4.3
B748	2929	137.2	4.0
B752	2667	54.7	1.5
Total			80.4

Considering feasibility, the increased climb duration of 1 to 3 minutes compared to the original flight can make the difference in being on-time or delayed. It is expected that this increased climb duration will be less important for long haul flights. One interesting result is that there is no significant flight time reduction difference between scenario 1 and 2. This means that a faster initial climb with a gradual decrease of calibrated-airspeed takes the same time as a constant CAS climb. However, the corresponding small difference in fuel benefits is proven to be significant. This shows that the constant CAS climb flown in current operations is indeed not the most optimal method to climb. In the future, this might be addressed with revised procedures or updated flight management systems and autopilots. Although it was shown that scenario 1 performed better than scenario 2 with the same flight time reduction, the question remains whether the fuel benefits justify the large increase in initial speed flown right after take-off. This higher speed postpones the distance at which the actual climb starts, causing higher noise levels in a larger area under the departure path. Considering the population density around Schiphol, this most likely does not justify the fuel benefits of S1 over S2.

Especially for heavy aircraft, the optimum climb speed is much higher than 250 knots. It was shown that for those types, the current speed constraint below 10000 feet has a large negative impact on the climb efficiency. On the other hand, optimum airspeed of the small to medium sized aircraft is only 20-30 knots above the current speed limit. The planes in this category (e.g. the B738, A320, E190) are responsible for 76 % of take-offs in 2017. Based on this, the recommendation for Schiphol would be to allow high-speed take-offs for these types since this would already significantly reduce the annual fuel consumption with a minimum violation of the current speed limit.

To answer the research question stated in the introduction: optimized continuous climb trajectories can indeed save at least 20 kg of fuel per flight using an operationally feasible climb profile. However, with the current regulations and restrictions, these profiles can not be flown.

X. RECOMMENDATIONS

The results presented in this study are found using various assumptions. Wind speed and direction have a large influence on the efficiency of a climb but was assumed -on average- to be zero for simulations using ADS-B data. The effect of this assumption can be assumed negligible, since the fuel consumption of the simulations are either under or overestimated depending on the wind direction. Due to the large number of flights analyzed in this study, these wind variations are predicted to cancel out. This prediction was partly proven true with the validation of the performance model in Table I. Assuming zero wind speed only increased the average fuel estimation error with 2.7%. A future study could include a weather model to estimate the TAS of ADS-B data. Also, several papers have proposed methods to predict

the mass of aircraft based on flight information [16] [17], which would greatly enhance the accuracy of ADS-B results. Furthermore, the thrust model used in BADA 3.12 only depends on altitude and not on airspeed. Although this is a frequently used assumption, the thrust decreases slightly with increasing airspeed. This will most likely impact the results in a way that the optimum initial acceleration speed and therefore the potential fuel benefit decreases. One possible thrust model that includes airspeed effects until Mach 0.4 is proposed by [18]. Finally, all climb profiles where flown by matching the Mach number at the end of the climb with the cruising Mach. A future study might investigate if this is indeed optimal.

Finally, it has to be mentioned that the interaction with other traffic has not been taken into account in this study. Real-life implementation of CCO and CDO operations at two US airports [5] [19] showed an increase in average fuel consumption due to longer lateral flight paths when facilitating both CCO and CDO. This paper leaves a gap for future studies to answer the question how CCOs would impact the airspace capacity and how CCOs and CDOs could be implemented in the current airspace structure. One recommendation for Schiphol would be to consider testing the results of higher initial acceleration speeds (e.g. 270 kts)

XI. Conclusion

This paper presented an approach to investigate the benefits of Continuous Climb Operations at Schiphol Airport. Using batch simulations, 481299 ADS-B flights and 17937 ACMS records from KLM have been analyzed. Based on ACMS data alone, reliable fuel savings could be estimated for 58.3 % of all take-offs in 2017. It was found that at least 6 million kg of fuel can be saved annually at Schiphol when aircraft climb using Cost-Index 0 and avoid ATC requested level-offs. These benefits increase with 46.4% to 11.2 million kg when aircraft no longer need to comply with the current speed restriction below 10000 feet. This deviates 8.2% from the theoretical optimum of 12.2 million kg that can be achieved when aircraft would fly variable CAS climbs. Furthermore, it was found that the 41.7% of other aircraft types have an annual fuel reduction potential of 8.0 million kg. Combined, this would also reduce 60.8 million kg of CO_2 emissions. The downside of these fuel savings is the prolonged acceleration phase after the NADP, violating the existing speed restriction. However, it was shown in this paper that several aircraft already climb according to this higher take-off speed. Recommendation have been made to allow these high-speed departures for all aircraft.

List of Symbols

γ	Flightpath Angle, Ratio of Specific Heats
ρ	Density of Air
a	Least-Squares Coefficient
C_D	Drag Coefficient Coefficient
C_{D_0}	Parasite Drag Coefficient
C_f	Thrust Coefficient
C_L	Lift Coefficient
C_{red}	Reduced Thrust Coefficient
C_T	Fuel Coefficient
D	Drag
f	Fuel flow
g_0	Gravitational Acceleration
h	Altitude
k	Induced Drag Coefficient
M	Mach Number
m	Mass
P_s	Excess Power
Thr	Thrust
V_{CAS}	Calibrated Airspeed
V_{GS}	Ground-Speed
V_{IAS}	Indicated Airspeed
V_{TAS}	True Airspeed
x	Ground Track Distance

References

[1] M. Miller, M. Graham, and J. Aldous, "Efficient climb and descent benefit pool," 2011.

[2] D. McConnachie, P. Bonnefoy, and A. Belle, "Investigating benefits from continuous climb operating concepts in the national airspace system: Data and simulation analysis of operational and environmental benefits and impacts," 2015.

[3] P. Melby and R. Mayer, "Benefit potential of continuous climb and descent operations," 2008.

[4] K. Roach and J. Robinson III, "A terminal area analysis of continuous ascent departure fuel use at dallas/fort worth international airport," vol. 3, 2010.

[5] M. Federal Aviation Administration, "2014 optimization of airspace and procedures for metroplex (oapm) houston metroplex post implementation analysis," *AIAA's 3rd Annual Aviation Technology, Integration, and Operations (ATIO) Forum*, 2015.

[6] ICAO, ""continuous climb operation (cco) manual"," 2013.

[7] M. Inaad, "Fuel and emission benefits for continuous descent approaches at schiphol," Unpublished M.Sc. Thesis, Faculty of Aerospace Engineering, Delft University of Technology, 2016.

[8] Eurocontrol. Base of aircraft data v3.12. [Online]. Available: https://www.eurocontrol.int/services/bada

[9] Y. Nakamura and K. Kageyama, "Study on validation and application of fuel-burn estimation," 2015.

[10] "Schiphol traffic review 2016," https://www.schiphol.nl/en/schiphol-group/page/traffic-review, accessed: 2017-07-03.

[11] J. Rosenow and F. Stanley, "Continuous Climb Operations with Minimum Fuel Burn," no. November, 2016.

[12] G. Ruijgrok, *Elements of airplane performance*, 2nd ed. Delft: VSSD, 2007.

[13] S. Hartjes and H. Visser, "Efficient trajectory parameterization for environmental optimization of departure flight paths using a genetic algorithm," *Proceedings of the Institution of Mechanical Engineers, Part G: Journal of Aerospace Engineering*, vol. 231, no. 6, pp. 1115–1123, 2016.

[14] J. Villarroel and L. Rodrigues, "An optimal control framework for the climb and descent economy modes of flight management systems," *IEEE Transactions on Aerospace and Electronic Systems*, vol. 52, no. 3, pp. 1227–1240, 2016. [Online]. Available: www.scopus.com

[15] R. Harmelen, K. Koch, "CO2 emission factors for fuels in the netherlands," *TNO Report R2002/147*, 2002.

[16] R. Alligier, D. Gianazza, and N. Durand, "Ground-based Estimation of the Aircraft Mass, Adaptive vs . Least Squares Method," *Tenth USA/Europe Air Traffic Management Research and Development Seminar (ATM2013) Airport*, pp. 1–10, 2013.

[17] J. Sun, J. Ellerbroek, and J. Hoekstra, "Bayesian inference of aircraft initial mass," *12th USA/Europe Air Traffic Management R and D Seminar*, 2017.

[18] M. Bartel and T. M. Young, "Simplified thrust and fuel consumption models for modern two-shaft turbofan engines," *Journal of Aircraft*, vol. 45, no. 4, pp. 1450–1456, 2008, cited By :12.

[19] L. Vempati, "Observed impact of traffic and weather on continuous descent and continuous climb operations," 2015, pp. 1C51–1C58.

Part II

Appendices

Appendix A

Level-off analysis

As mentioned in the paper in Part I, a distinction was made between procedural level-offs (due to abatement procedures and speed restrictions) and supplemental Air Traffic Control (ATC) level-off requests. This will be referred to as type 1 and type 2 inefficiencies respectively. Type 2 level-offs are interesting to further investigate, since these inefficiencies are unintended and caused by traffic density problems or other reasons.

A-1 Annual variations Type 1 and Type 2 level-off

The occurrence of type 1 and 2 level-offs varies throughout the year. All recorded inefficiencies are grouped by hour, day, week and month as shown in Figure A-1. Each flight can level-off more than once. Therefore, the vertical axis only shows the number of level-offs and not the number of flights.

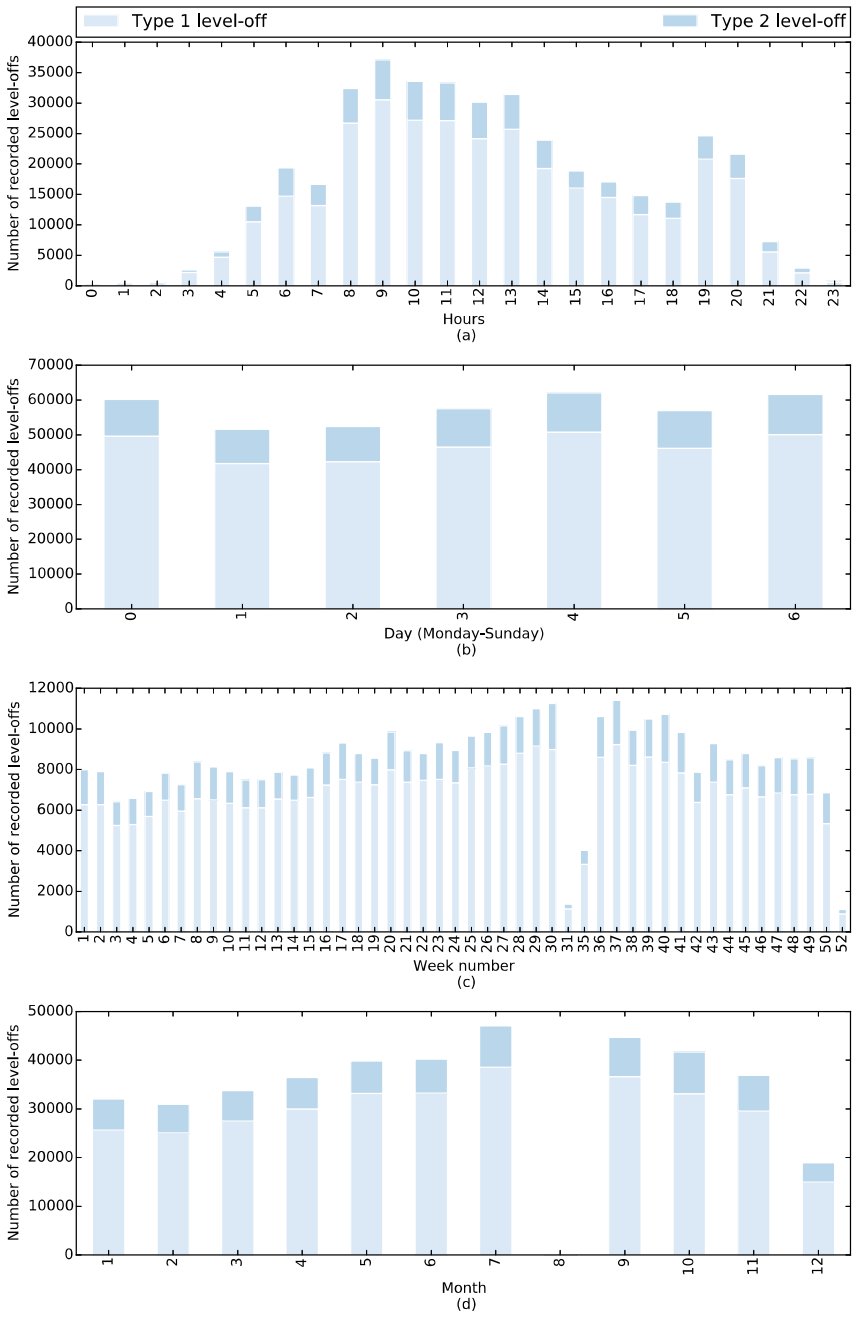

Figure A-1: Hourly (a), daily (b), weekly (c) and monthly (d) variation in level-offs. August and December are partly missing

A-2 Level-off locations Type 2 between 3000-8500 ft

Figure A-2 shows the location of type II level-offs between the 3000 and 8000 ft. The red lines indicate the standard departure routes currently used at Schiphol. Other altitude ranges are shown in Figures A-3 to A-6.

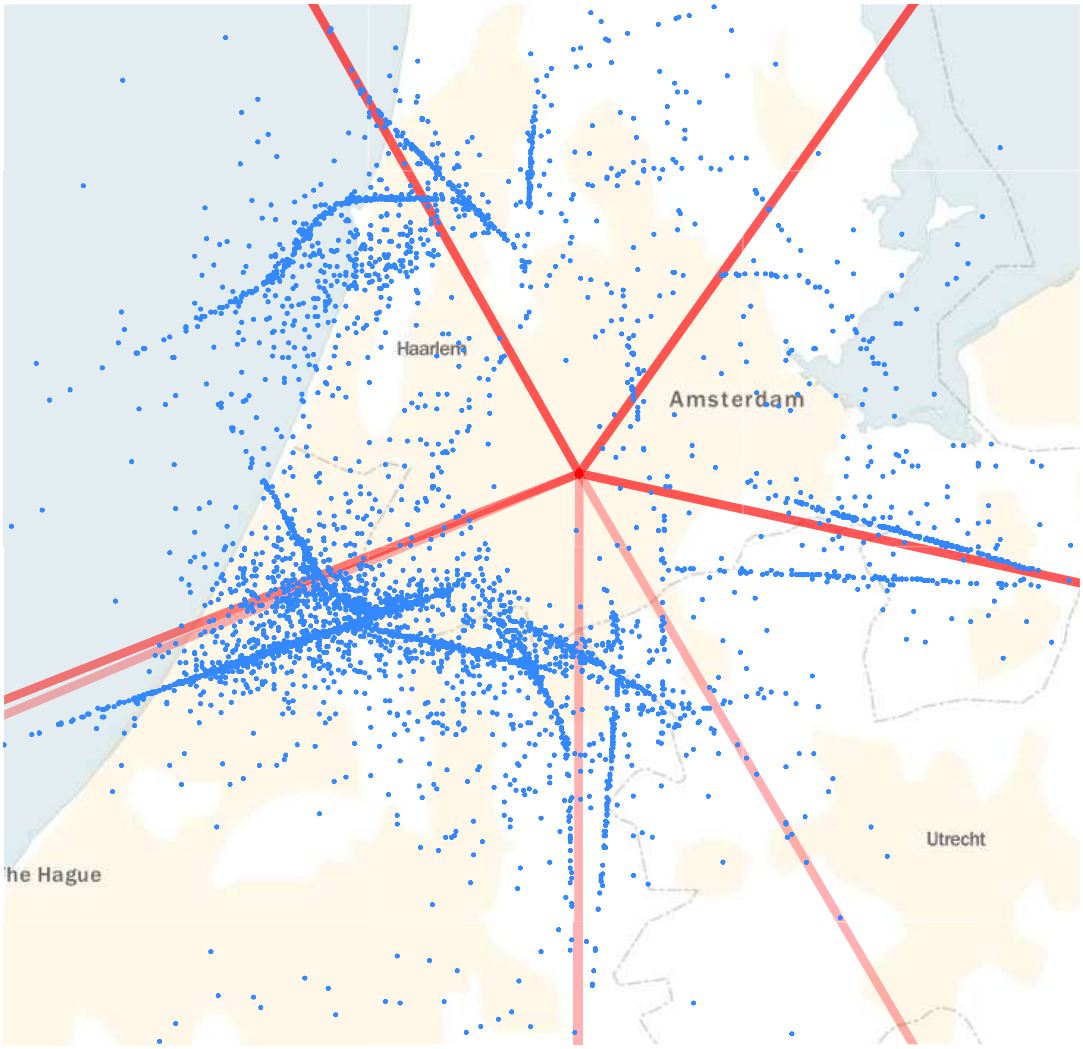

Figure A-2: Locations of type 2 level-offs between 3000 and 8000 ft.

A-3 Level-off locations Type 2 between 12500-20000 ft

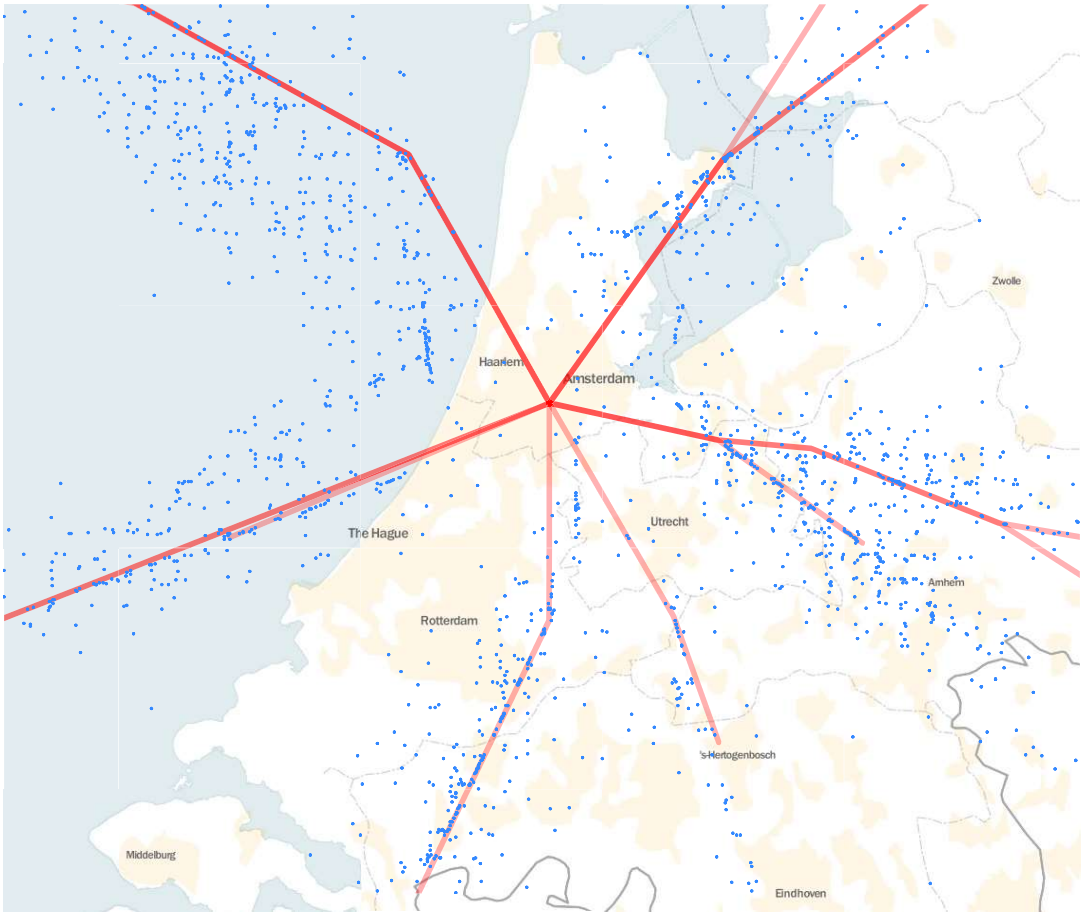

Figure A-3: Locations of type 2 level-offs between 125000 and 20000 ft.

A-4 Locations Type 2 between 20000-27000 ft

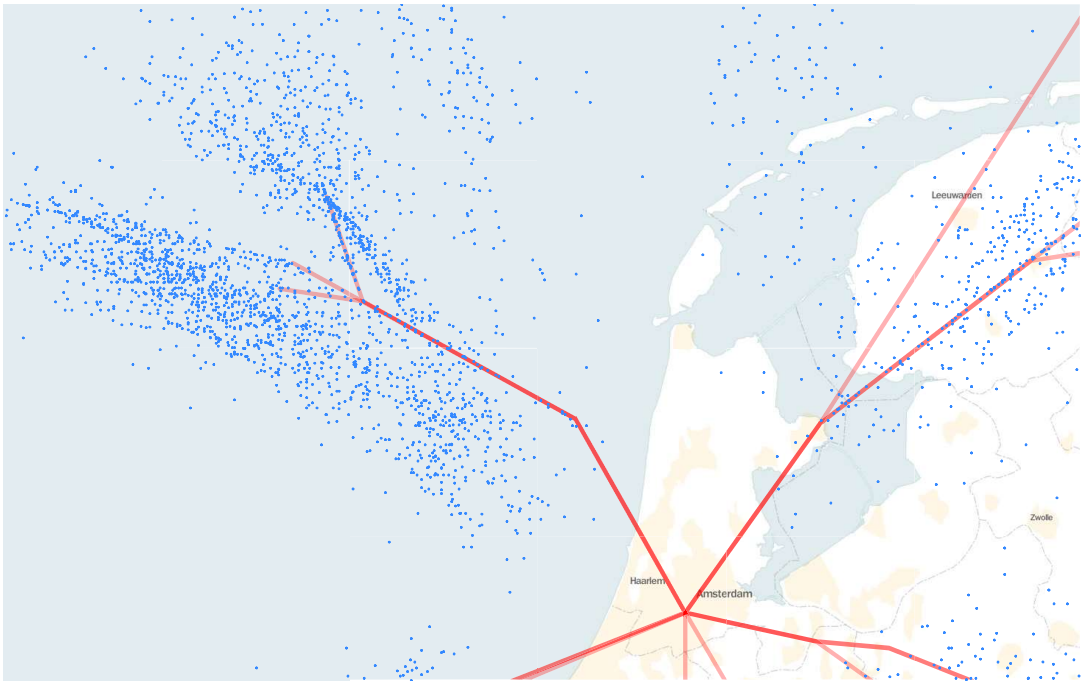

Figure A-4: Locations (North) of type 2 level-offs between 20000 and 27000 ft.

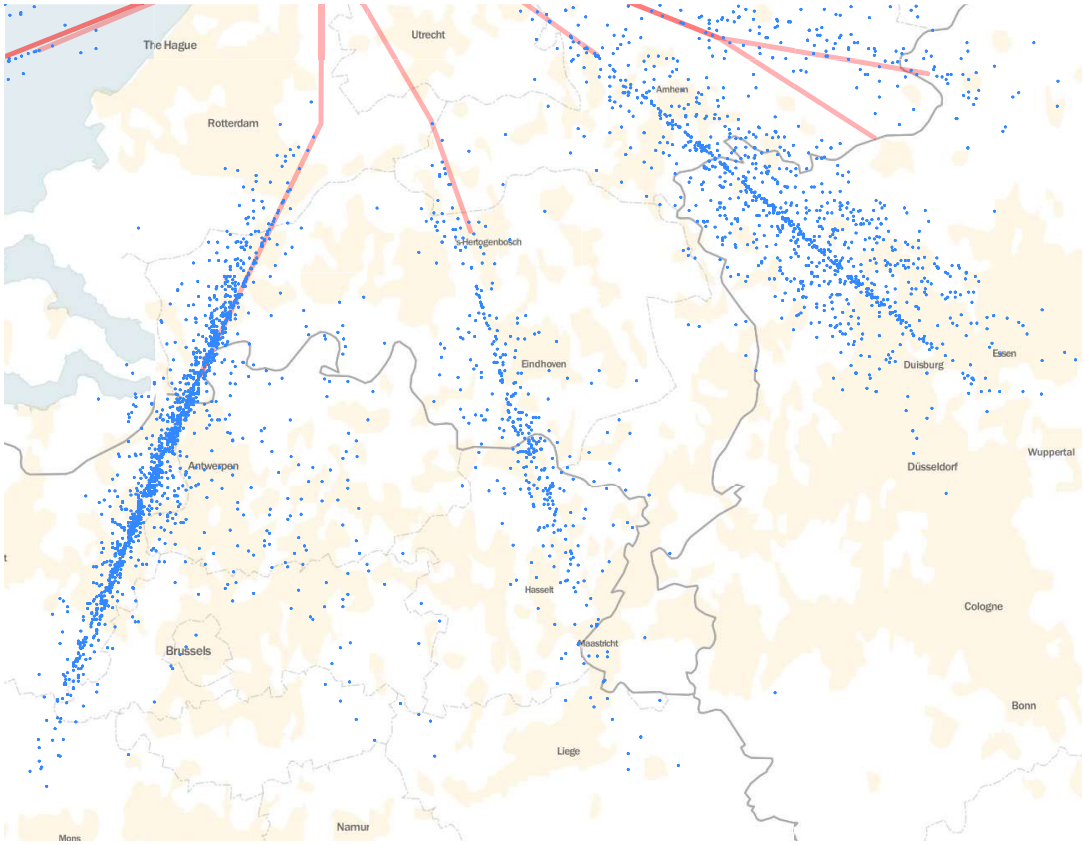

Figure A-5: Locations (South-East) of type 2 level-offs between 20000 and 27000 ft.

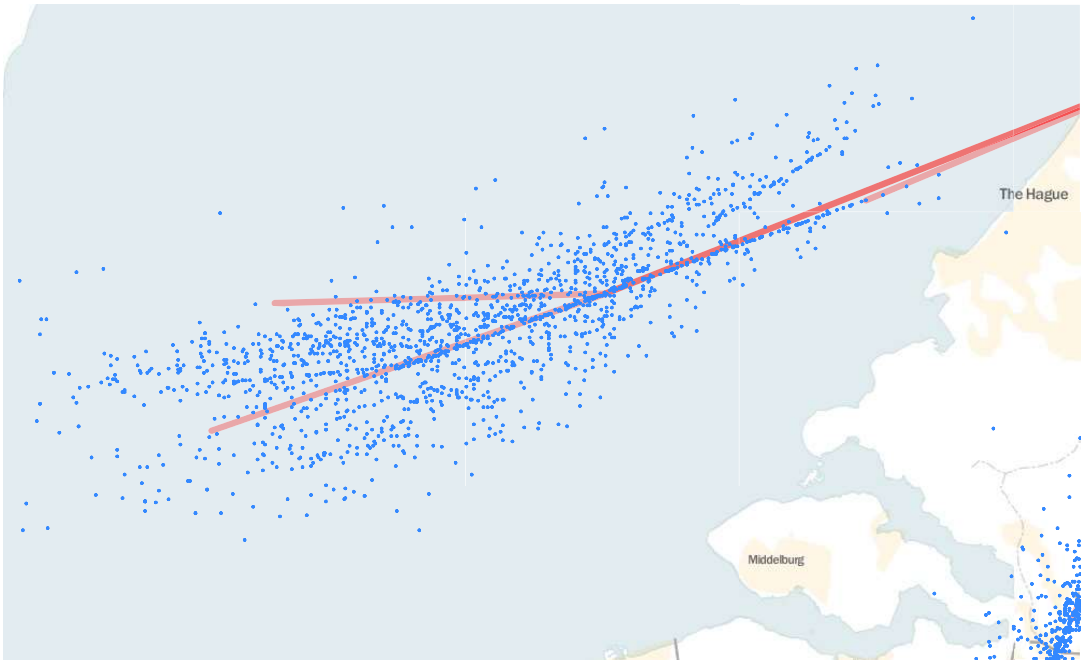

Figure A-6: Locations (South-West) of type 2 level-offs between 20000 and 27000 ft.

Appendix B

Code structure

The code used for this thesis has been organized in several modules. These modules feed the main scripts `mainframe_klm.py` and `mainframe_adsb.py`. A flowchart of this process is presented in Figure B-1. Table B-1 lists the content of the modules and a short description. A detailed overview of the data-sources can be found in Part III.

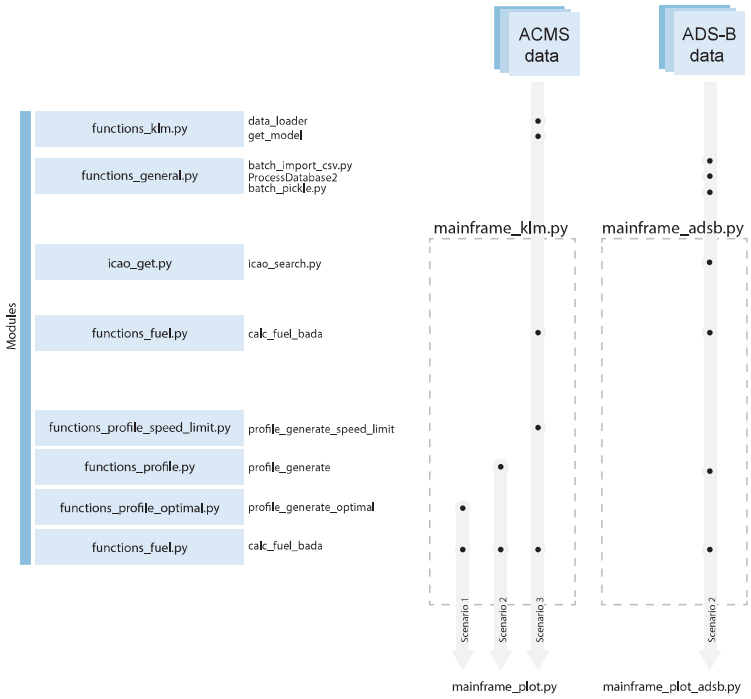

Figure B-1: Overview of code structure

Table B-1: List of modules with corresponding functions and descriptions

Module	Function	Description
functions_general.py	constants (class)	Create object with constants
	unix_ts_to_seconds	Convert entire array of UNIX EPOCH timestamps to datetime and extract the seconds
	tas_to_cas	Convert either list or value from TAS to CAS using density and pressure
	tas_to_cas_h	Convert value of TAS to CAS using altitude
	get_isa	ISA calculate density pressure and temperature using height
	get_isa_multi	vectorized version that calls get_isa.py
	ProcessDatabase2	Filter flights based on departure Schiphol and store in pickles. Function is called by batch_pickle
	time_level	Create altitude and velocity spectrum used to detect level-offs
	interp_adsb	Interpolator for ADS-B data, ignoring NaN values
	is_outlier	Outlier detection for detecting peaks in altitude and velocity spectrum created with time_level
functions_fuel.py	calc_fuel_bada	Estimate fuel consumption using BADA coefficients
functions_klm.py	data_loader (class)	Load and pre-process ACMS .csv file to create object with flight data
	get_level_flag	Adapted version of function time_level to analyze level-offs in ACMS data
	get_model	Obtain aircraft model based on tail number
functions_profile_optimal.py	profile_generate_optimal	Climb profile generator for scenario 1. Simulating climbs according to optimal TAS settings
	dv_dh_speed	Determine the required optimal speed at each altitude based on the coefficients found in dv_dh_coefficients
	dv_dh_acceleration	Determine the required dv_dh at each altitude based on the coefficients found in dv_dh_coefficients
	dv_dh_coefficients	Determining the rate of speed change dV_{TAS}/dh required when climbing. The coefficients of an OLS fit of optimal TAS change with altitude are returned.
functions_profile.py	profile_generate	Climb profile generator for scenario 2. Climbs are flown using constant CAS settings
functions_profile_speed_limit.py	profile_generate_speed_limit	Climb profile generator for scenario 3. Adjusted version of profile_generate including speed limit.
icao_get.py	icao_search	Search registration id, model, ac type and operator based on ADS-B ICAO in database
	icao_update	Update database
tools.py	batch_import_csv	Batch convert each day of decoded ADS-B .csv data into .db format
	batch_pickle	Batch filter .db files by departures Schiphol and store in pickles
	pickle_merger	Merge result pickles
	txt_to_csv	Convert raw ACMS files to .csv

Part III

Preliminary thesis report

Continuous Climb Operations at Schiphol

Preliminary Thesis Report

Preliminary Master of Science Thesis

For obtaining the degree of Master of Science in Aerospace Engineering
at Delft University of Technology

J. Klapwijk

2 February 2018

Faculty of Aerospace Engineering · Delft University of Technology

Delft University of Technology

Delft University Of Technology
Department Of
Control and Simulation

Dated: 2 February 2018

Readers:

dr.ir. J. Ellerbroek

Prof.dr.ir. J. M. Hoekstra

Ceriel Janssen (KLM)

Acronyms

ACMS	Aircraft Condition Monitoring System
ADS-B	Automatic Dependent Surveillance Broadcast
ATC	Air Traffic Control
BADA	Base of Aircraft Data
BoC	Begin of Climb
CAS	Calibrated Airspeed
CCO	Continuous Climb Operations
CDA	Continuous Descent Approach
CDO	Continuous Descent operations
CI	Cost Index
EDP	Expedite Departure Path
ESF	Energy Share Factor
FAA	Federal Aviation Administration
GS	Ground Speed
IAS	Indicated Airspeed
ICAO	International Civil Aviation Organization
ISA	International Standard Atmosphere
KLM	KLM Royal Dutch Airlines
MSE	Mean Squared Error
MTOW	Maximum Take-off Weight
NADP	Noise Abatement Departure Procedure
OEP	Operational Evolution Partnership
OPF	Aircraft Performance Operational File
RNAV	Area Navigation
SID	Standard Instrument Departure
STAR	Standard Arrival Route
TAS	True Airspeed

TEM Total-Energy Model
TMA Terminal Manoeuvering Area
ToC Top of Climb
ToD Top of Descent

Contents

List of Figures

List of Tables

Chapter 1

Introduction

Reducing fuel, noise and emission are more important than ever in aviation. Not only by improving the design of an aircraft but also by optimizing its operations. One of the ways to achieve this is by improving the efficiency of climb and descent phases of flight. Because of the stair-step procedures followed by air traffic control and the transitions between airspace sectors, climb and descent phases of a flight are likely to contain horizontal segments (level-offs). Continuous Climb Operations and Continuous Descent Operations aim at removing these levels-offs.

Continuous descents have been the subject of many studies in the past, mainly due to the fact that the frequency and duration of level-offs is larger during landing than take-off (Miller, Graham, & Aldous, 2011). Despite of this preference, previous research has shown that continuous climb trajectories do have potential to reduce fuel consumption McConnachie, Bonnefoy, and Belle (2015) Melby and Mayer (2008) Miller et al. (2011). However, no studies have been conducted that asses the continuity of climbs at Schiphol Airport in the Netherlands.

Although the climb procedures at Schiphol are considered close to continuous already, there are some inefficiencies visible at key altitudes. The goal of this research is to find the origin of these level-offs and investigate the potential fuel-benefits of 100% continous climb operations at Schiphol. In addition, a concept solution to implement CCOs and CDOs at Schiphol will be investigated.

The results of this study will indicate if the benefits of Continuous Climb Operations (CCO) are significant enough to justify change of current procedures at Schiphol. In a broader context, the objective of this research will be in line with the international efforts (e.g., SESAR, NextGen) [1][2] to introduce and deploy CCOs and CDOs in concept ATM solutions.

[1] http://www.eurocontrol.int/service/continuous-climb-and-descend-operations
[2] http://www.sesarju.eu/sites/default/files/documents/news/4.2_SESAR_NextGen_Interop_v1.pdf

Chapter 2

Literature Review

In the last decade, research on flight efficiency became more relevant than ever due to an increase in fuel cost. Studies related to the climb phase range from quantifying cost associated with level-offs to 3D climb optimization. This literature study will position the current study in relation to previous work done. First, a brief overview of the differences between CCO and Continuous Descent operations (CDO) research will be given. Next, a brief summary of related studies, both simulated and empirical, will be presented. The section continues with a discussion on the definition of continuous climb. Finally, the section will present the current knowledge gap in CCO research and the contribution of this study to the body of knowledge.

2-1 Continuous Climb versus Continuous Descent

Unlike the descent phase of flight, the climb phase has not yet been studied in great numbers. Since arriving aircraft more often experience lengthy low-altitude level-offs, the benefits in terms of fuel reduction, noise and emissions of a Continuous Descent Approach (CDA) are more evident. However, it was suggested by McConnachie et al. (2015) that due to the high thrust settings and large take-off weight during climb, optimization of climb operations also has potential to significantly reduce fuel consumption. The study of continuous climb is absolutely not identical to the descent, but what makes a CDO different from a CDA?

During landing, aircraft in the terminal area are spaced and sequenced at strategic heights by Air Traffic Control (ATC). When the airport demand peaks, airplanes are frequently placed in level holding patterns. This, together with the interception of the glide slope often requires horizontal flight during descent. A different strategy is used for take-off. Before departure, aircraft are spaced and sequenced on ground using separation standards. After take-off, planes diverge and accelerate. According to Melby and Mayer (2008) this decompression effect is one of the reasons why todays operations often experience near continuous climb performance as opposed to descent.

When investigating a fuel-optimal CDA, one needs to determine the Top of Descent (ToD). After this point, the engine thrust setting is reduced to idle and the aircraft follows an ideal

glide path to the runway threshold. Variables to consider are flight path angle and ToD.

In order to find a fuel-optimized CCO, one needs to find the optimal combination of thrust settings, airspeed and flightpath angle γ. These variables are dependent on aircraft type, weight, real life weather conditions and -when adding even more complexity- the Cost Index (CI) setting used by airline operators (Jung & Isaacson, 2003). As explained by Dalmau and Prats (2015): "This factor reflects the relative importance of the cost of time with respect to fuel cost". Furthermore, the majority of take-offs nowadays are done using reduced thrust to lessen engine wear. Finally, take-off performance is often limited due to noise abatement procedures and speed restrictions below certain altitudes (Rosenow & Stanley, 2016)

From a controller's perspective, the design of both CCO and CDO procedures should consider the effects of re-routing and vectoring. For a given CDO, path shortening could lead to dangerous situations since the aircraft is descending at a much steeper path than a conventional descent. The opposite is true for CCOs, where path shortening could lead to reduced flight time, hence less fuel consumption. Path lengthening during a continuous climb eventually leads to larger time spent at cruise altitude while lengthening during continuous descent requires the aircraft to level-off or change flight path angle.

2-2 Results of previous work

Over the past decades, many researchers have investigated climb and descent operations. Research on the climb phase of flight is mostly done by simulations using radar data, although some actual implementation results are available. This section will briefly discuss the most relevant results in chronological order.

2-2-1 Analyzing radar data

One of the first studies on both CCO and CDO operations was performed by Melby and Mayer (2008). Using radar track data from 34 Operational Evolution Partnership (OEP) airports in the United States it was found that continuity of climb and descent phases could potentially lead to a total benefit of $380 million annually. From this, only 8 percent can be associated with climb operations. In order to quantify this they assumed that level flight segments below cruise altitude are sub-optimal because of reduced speed, higher air densities and longer flight times. With this in mind, the benefits were calculated by comparing the fuel consumption of a level flight segment with the fuel burn of a comparable segment at cruise speed and altitude. The fuel burn was estimated using a Base of Aircraft Data (BADA) based performance model assuming clean aircraft configuration, idle thrust descents and true airspeed equal to ground speed recorded by radar. The assumptions used for climb phases (e.g. if the BADA reference mass was used) are not stated. It has to be further noted that the annual benefits where calculated by interpolating a single day of radar data. By doing so, the effect of traffic density variations during the year are not taken into account. Finally, it has to be noted that more than half of the $380M potential benefits where associated with flight time reduction and not by reduced fuel consumption. To quantify this, Melby and Mayer used an Aircraft Direct Operating Cost estimate to asses the crew and maintenance cost per flight minute.

In 2010, after implementation of CDA procedures at Dallas/Fort Worth International Airport, Roach and Robinson III (2010) investigated the impact of new CDA arrival routes on climb operations. In the old situation, the altitude of arrivals streams imposed climb restrictions on departing traffic. These restriction where causing level-flight segments in 20% of all departures. Because of the elevated approach path of CDA tracks, CCO flights where suddenly a possibility. Based on radar data, 9 days with a total of 3,836 climbs where analyzed. Level flight segments below cruise speed and altitude where replaced with the same segment at cruise conditions. Fuel estimations where performed using the BADA performance model. Based on this, a potential average fuel reduction of 7 gallons per flight was estimated. Interestingly, the study concluded that continuous descents have a beneficial effects on the use of continuous climbs. This supports the objective of current research to design a concept solution implementing continuous operations at Schiphol.

Roach's study was based on earlier work done by Jung and Isaacson (2003) at the same Dallas/Forth Worth airport. The aim of their work was to add unrestricted climb functionality to the existing Expedite Departure Path (EDP) tool developed by NASA. This tool is used to predict and schedule departure paths in order to advise air traffic controllers. It was found that accurate prediction of climb trajectories was a major challenge, due to the uncertainty of aircraft weight, airline procedures and wind prediction. Although the report identified potential benefits of CCO, including reduced fuel burn and time-to-climb, exact numbers where not given yet.

A different study in the USA, conducted by Miller et al. (2011), investigated the potential benefits of optimized climb and descent paths using NASA's strategic Arrival Manager (AMAN) and multi-climb tool. These tools facilitate optimum continuous climb and descent trajectories while maintaining safe separation from other traffic. Both current and future (2020) traffic scenarios where simulated. The expected annual fuel savings for CCO turned out to be $42 Million, which is roughly 8 times lower than the expected $355M savings of CDO. In a similar fashion as Melby, Miller calculated the benefits of using CCO and CDO by comparing the fuel consumption of a level-off with that of a similar stretch at cruising altitude. This way, the assumption was made that the level flight segment would otherwise be flown at cruising altitude. It has to be noted that altitudes under 10000 ft. where not covered during this study Miller et al. (2011).

In 2015, McConnachie et al. (2015) performed one of the few studies purely focusing on the benefits of climb continuity by analyzing data from two different sources. The Performance Data Analysis and Reporting System (PDARS) and the Enhanced Traffic Management System (ETMS). While PDARS obtains its information using radar data the ETMS relies solely on position and altitude messages sent by aircraft. Over a period of one year, 20 days of data was collected and fuel consumption simulated using the Federal Aviation Administration (FAA)'s Aviation Environmental Design Tool (AEDT). New CCO profiles were constructed by removing the level flight segment nodes from the radar track data and match the climb rates of the remaining initial and final nodes. The results indicated an average fuel reduction ranging from 6- 19 kg per flight. Also, it was found that 30% of the flights experience a level-off during climb and the majority of level-offs last less than 1 minute. Furthermore, the altitudes at which aircraft level- off seems to be uniformly distributed with peaks at terminal

area ceilings and sector transitions.

2-2-2 Emperical results of CCO implementation

In May 2014, Houston George Bush Intercontinental Airport and Houston Hobby Airport implemented 12 new Area Navigation (RNAV) Standard Instrument Departure (SID)s and 10 RNAV Standard Arrival Route (STAR)s. The primary goal of this change was to remove level-off sections during descent and to facilitate CCO and CDO procedures at both airports. Almost half a year after implementation, Post-analysis performed by the Federal Aviation Administration (2015) concluded that the change in average fuel consumption per flight ranged from -6.2 to -13.4 gallons for the descent phase and -0.2 to +12.5 gallons for the climb phase. Interestingly, the new climb procedures used more fuel compared to the old situation in some cases. This result was partially explained by the increased path length of the new departure routes.

Besides the post-analysis, Vempati (2015) used the new SIDs and STARs to study the influence of weather and demand on the execution of CCO and CDO operations. It was concluded that holding activities and weather conditions/restrictions have the largest influence on the occurrence of CCO and CDO. However, the impact on CDOs is larger than the impact on CCOs. This is explained by the fact that during bad weather conditions, departing flights are delayed on ground, while arriving planes are placed in holding patterns.

2-3 Defining Continuous Climb Operations

As can be read in the CCO manual ICAO (2013), the International Civil Aviation Organization (ICAO) officially defines a CCO as:

"An operation, enabled by airspace design, procedure design and ATC, in which a departing aircraft climbs without interruption, to the greatest possible extent, by employing optimum climb engine thrust, at climb speeds until reaching the cruise flight level."

In other words, to execute an official CCO the aircraft needs to continuously climb according to a path optimized for the aircraft. The official definition does not explicitly state a minimum climb rate or airspeed since this is aircraft specific. The general idea is to design the airspace such that it allows aircraft to use their in-flight techniques to optimize the climb profile. Regarding this profile, the ICAO manual states:

"The optimum vertical profile takes the form of a continuously climbing path. Any non-optimal climb rate segments during the climb (other than during the Noise Abatement Departure Procedure (NADP)) to meet aircraft segregation requirements should be avoided."

Furthermore, the manual suggests to carefully consider the influence of NADP, speed restrictions, and arrival streams in the design of the departure routes. In case level-flight is unavoidable, the manual states:

"Level segments where there are also speed constraints result in much more severe operational constraints than where level flight occurs when there is no speed constraint. This provides further incentive to avoid level flight segments where speed constraints exist."

Summarizing, a continuous climb is defined as a climb optimized for aircraft characteristics. Continuous Climb Operations is the facilitation of this climb by means of airspace, controller and airplane interactions

2-4 Defining a level-off

In order to quantify and detect any deviations from a continuous climb path, it is necessary to define an inefficiency or level-off. In each of the studies presented in Section 2-2, different methods where used to detect level-offs, a brief overview is given below:

- Melby and Mayer (2008) used a "Time-in-Level-Flight" metric. At various nominal altitudes, this metric recorded the time required to climb 100 ft. These values where averaged and the result is an altitude spectrum in which level-off altitudes, climb performance and average time in level flight can be read.
- McConnachie et al. (2015) defined an level-off inefficiency as a climb rate below 1000 ft per minute while the aircraft is flying below 80 percent of the Top of Climb (ToC) altitude.
- Miller et al. (2011) considered the climb and descent phase between 10000 ft and 85% cruising altitude. To determine a level-off, Miller used a double threshold method. First, the algorithm searched for one minute of consecutive datapoints which are bounded by $\pm$100 ft per minute climb rate. Next, the start and endpoints of the level-off where determined by searching the first and last datapoint bounded by $\pm$200 ft/min climb rate. Afterwards, level-offs with a duration shorter than 1 minute or longer than 20 minutes where disregarded.
- Vempati (2015) used a similar approach in level-off detection. The ToC and ToD where determined using the highest measured altitude within 200 nm of both departure and arrival airports. With the climb phases distinguished, a level-off was then defined as a maximum altitude difference of 200 ft during at least 50 seconds.

It is expected that the majority of level-offs at Schiphol Airport have a short duration and do not often reach a zero rate of climb. To detect these subtle inefficiencies, a method such as the one presented by McConnachie or Melby will likely provide better results than the method used by Miller or Vempati. In this study, a level-off will be defined as:

A section of the climb between Begin of Climb (BoC) and 80% of ToC in which a rate of climb lower than 1000 ft/min is experienced that is not in line with the average rate of climb.

2-5 Benefits and disadvantages of CCO

Reducing fuel consumption is the most evident reason to implement continuous climb operations. Table 2-1 summarizes the results found in Section 2-2. The papers from both Melby and Miller only stated total annual fuel savings. Therefore, conversions to kg per flight are

Table 2-1: Summary of CCO fuel benefits found by previous studies

Study	Fuel benefit	Unit	Airports/Location	Method
Melby and Mayer (2008)	~2	kg / flight	34 OEP airports, US	level-off removal
Roach and Robinson III (2010)	22	kg / flight	Dallas Fort Worth, US	level-off removal
Miller et al. (2011)	~3.5	kg / flight	35 OEP airports, US	simulate optimal trajectories above FL010
Federal Aviation Administration (2015)	-39 to 0.2	kg / flight	2 airports, US	CCO implementation results
McConnachie et al. (2015)	6 to 9	kg / flight	3 airports, US	level-off removal

estimated using the data available in the papers. The large spread in results can be explained by the different approaches used. Some papers only considered busy airports with frequently occuring level-offs while the scope of other papers was nation wide. Also, the methods to determine fuel savings differ between the various studies.

Results have shown that, although the fuel savings are likely to be lower than a CDA, the implementation of a CCO will be easier and the possibility of execution is higher compared to CDA. Considering the distance traveled over ground, altitudes below 10000 ft are usually flown at lower speeds due to airspace restriction. According to Melby and Mayer (2008) CCOs can reduce the flight time in these lower speed conditions, hence result in shorter overall flight times.

Besides fuel reduction additional improvements in noise, efficiency and congestion can be achieved Jung and Isaacson (2003). Finally ICAO expects a reduction of workload due to a reduced number of ATC interventions and radio transmission.

On the other hand, Hartjes and Visser (2016) concluded that a compromise between noise and fuel efficiency does not always result in a CCO profile. Furthermore, it was shown by Vempati (2015) that -although a continuous climb might improve fuel consumption- it also negatively influences the capacity of an airport under certain conditions. Depending on the type of implementation and the priority of CCO compared to CDO, fuel consumption might increase as shown by the Federal Aviation Administration (2015)

2-6 Analysis: bridging the gap

Several studies in the past have investigated the benefits of continuous climb in the US airspace. In most cases, level-off sections of more than a minute where found in historic flights. Until now, most research simply removed level-flight sections to calculate fuel benefits. This way, rate of climb and airspeed during take-off remain unchanged and un-investigated. The situation at Schiphol Airport is different since it is expected that the majority of flights already execute a near-continuous climb. The current study will therefore investigate if improvements can be made that further optimize climb procedures and decrease fuel consumption. In other words, to better understand what the effects are of restrictions and regulations and how current-day operations deviate from a fuel-optimized climb. In addition to most research using only historic radar data, this study will also make use of ACMS data provided by KLM Royal Dutch Airlines (KLM). Variables such as mass, temperature and wind are usually not available when using radar data but greatly improve the accuracy of simulations.

2-7 Conclusion

Previous CCO research has shown the potential to reduce fuel consumption, noise and emissions. It was shown that CCO could result in a reduction between 2 and 22 kg per flight, depending on airspace design and traffic density. Although the ICAO describes the general idea behind a continuous climb, the parameters that determine the climb profile are left to the end user. The goal of this study is to find the benefits of CCO operations when flying fuel optimized climb trajectories. Although in everyday operations this might not be realistic, this ideal scenario could give insight in how much current operations at Schiphol deviate from a fuel-optimized climb trajectory. This in turn can quantify the impact of Schiphol's airspace design, procedures and regulations on the consumption of fuel.

Chapter 3

Research Plan

The research objective is to investigate the potential benefits of 100% continuous climb operations at Schiphol by comparing historical flight data with simulated optimal continuous climb profiles. Also, a concept solution will be investigated to implement CCOs and CDOs at Schiphol, without compromising on current performance, noise and safety.

3-1 Research Questions

In order to achieve this objective, the following research questions and sub-questions need to be answered during this project:

What are the potential annual fuel benefits if all flights at Schiphol would take-off using an operationally optimal continuous climb profile compared to the current baseline operations?

- What is the baseline fuel consumption of all flights departing Schiphol?
- What is an operationally optimal climb profile?
- What is the estimated fuel consumption when all baseline flights climb optimal continuous climb profiles?

How can CCOs and CDOs be embedded in the current Terminal Control Area (TMA) structure of Schiphol, without compromising on performance, noise and safety?

3-2 Research Objectives

In order to answer the research questions, the following objectives are formulated:

- Define a level segment/inefficiency

- Analyze the variations in level segments/inefficiencies during a year
- Identify inefficiencies in current-day operations
- Determine the number of ADS-B recorded flights required to represent all annual take-offs at Schiphol
- Calculate the error and deviation between the BADA fuel-model and actual fuel consumption during the climb phase
- Assess the impact of the assumptions used in the BADA fuel-model.
- Determine how to model and calculate optimal climb profiles
- Investigate the influence of the current Terminal Manoeuvering Area (TMA) on the execution of CCOs and CDOs
- Determine the limiting factors, restrictions and requirements for continuous climb and descent at Schiphol.
- Investigate feasible trajectories for CDOs and CCOs at Schiphol, taking into account the limiting factors, restrictions and requirements.

The novelty of this research is to quantify the potential annual cost reduction for flights taking-off from Schiphol and hereby not only investigate the removal of level segments but also consider optimal climb paths and a feasible implementation at the airport.

3-3 Work flow

The basis of this research proposal fits within the theory-testing and partly within the design-oriented research domain. The hypothesis to be tested is:

Optimized continuous climb trajectories will on average save at least 20 kg of fuel per flight over current-day operations at Schiphol airport.

The design-oriented part will assume that continuous climb and descent operations are beneficial, and a concept implementation has to be investigated.

A work breakdown structure can be seen in Figure 3-1. In line with the planning and research questions, the first part of this study will consist primarily of literature research. Familiarization with previous work will establish the basis for data analysis. This includes the definition of level-off sections, recognition of flight phases and necessary assumptions. The literature study will also dive into restrictions and procedures at Schiphol. This includes velocities, altitudes, climb rates and noise abatement procedures.

Initial analysis of ADS-B data will be performed to investigate the altitude, frequency and cause of climb inefficiencies in the first half of 2017. This will result in optimization opportunities, hence scenarios which will later be compared to the baseline fuel consumption. The hourly, daily and monthly variations will be analyzed to assess if extrapolation of results will be possible. Research on fuel-optimized climb will serve as basis for a 2D vertical trajectory

model. This model will calculate valid trajectories for each aircraft based on the boundary conditions, assumptions and scenarios found.

Parallel to this, the BADA model needs to be implemented and validated using actual flight data recorded by aircraft (Section 3-5). The validated model will be used to analyze both historic flights as well as the trajectories found by the climb trajectory model.

Based on the results obtained, an assessment will be done on the impact of CCO profiles in the current airspace structure.

3-4 Planning

A Gantt Chart visualizing the planning of this thesis project can be found in Appendix D.

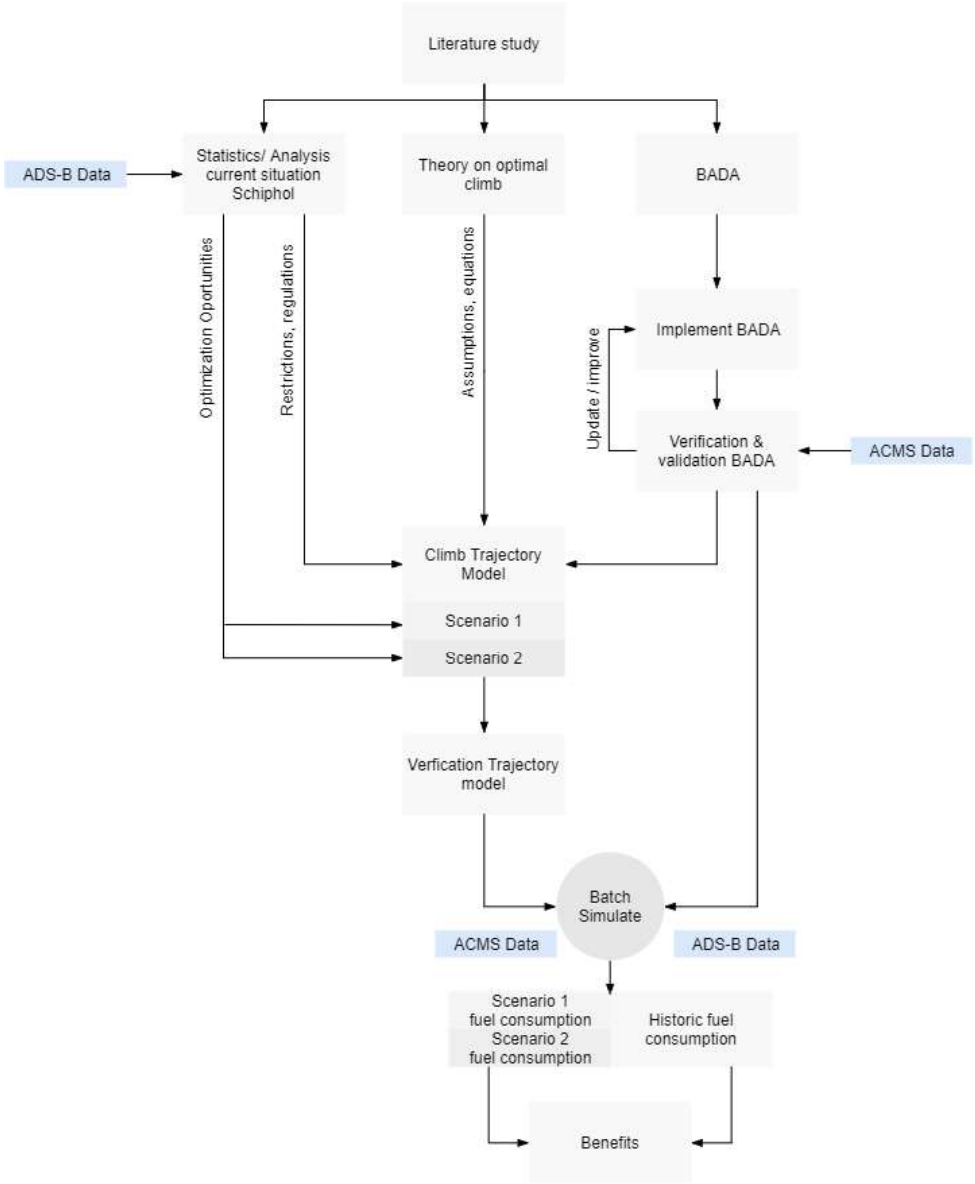

Figure 3-1: Work Breakdown Structure

3-5 Data

In order to scope the research and limit the amount of data, flight records between 1-1-17 and 1-9-17 will be considered. Although earlier data is available, the 2017 records will give insight in the most recent situation at Schiphol airport.

Two sources of flight data are available for this Thesis. The majority of flights is covered by ADS-B radar data which contains only basic information such as location, altitude and speed. A part of these flights will have additional ACMS data provided by KLM. This airline was responsible for 63.4% of the flight movements at Schiphol last year, according to the *Schiphol Traffic Review 2016* (n.d.).

3-5-1 ADS-B radar data

The ADS-B data transmitted by aircraft can be received using a commercially available ADS-B receiver. At TU Delft's faculty of Aerospace Engineering they continuously record these transmissions. Decoding of the messages is done using the open-source work of Sun [1].Table A-1 in Appendix A shows the variables available. The ICAO aircraft address can be translated in aircraft model, airline and registration using a look-up table.

3-5-2 KLM ACMS data

The aircraft condition monitoring system was originally developed to improve engine and maintenance operations. Later, this system became part of the mandatory flight monitoring to investigate if operational limits are exceeded. Which variables are monitored depends on aircraft type and age. In general, most parameters are recorded every second. Some variables however, are recorded with a 4 seconds interval. Similar to the ADS-B data, interpolation will be used to change the interval to 1 second. Table A-1 in Appendix A shows the list of variables that will be available. The recordings start after the take-off roll until a few seconds after ToC. Several aircraft have a deviating parameter-set and their data will not be analyzed. Radio altitude is only valid until 2500 ft. Ground speed is calculated on-board using the measured wind speed, direction and true airspeed is unreliable in the first seconds after take-off.

3-6 Limitations and Assumptions

For this research, only aircraft equipped with jet engines will be regarded. Also, only the vertical 2-D plane will be considered. When using ADS-B data, the assumption will be made that there is no wind. As a result, ground speed equals true airspeed. Finally, flights will assume International Standard Atmosphere (ISA) with zero temperature and pressure deviation.

[1] `https://github.com/junzis/adsb-decode-guide`

Chapter 4

Methodology

This chapter will elaborate on the simulation methods used in this study and is structured according to the work-breakdown structure in Figure 3-1. First, a data analysis will be presented that identifies any inefficiencies in todays operation. The next section explains how Eurocontrol's BADA model will be used and validated. Finally, a model to optimize and simulate climb trajectories will be explained and validated.

4-1 Current Operations at Schiphol

In this section, an overview will be given of the take-off procedures and regulations. The section will conclude with an analysis of the current airspace efficiency.

4-1-1 Airspace Structure, Departure Routes and Regulations

Schiphol has a total of 12 runways (6 unique) with each 5 to 13 assigned SID routes. These routes are considered minimum noise routes and try to avoid populated areas. The SID routes are constructed with the waypoints shown in Figure B-1.

The majority of flights is expected to depart using NADP2. This procedure is described by ICAO Doc 8168 Volume I. At 1500 ft, the plane should decrease the body angle while keeping positive rate of climb to reach flaps-up speed and retract flaps. In the NADP1 procedure, this acceleration is performed at 3000 ft.

After the noise abatement procedure the speed of departing aircraft is limited to 250 kts Indicated Airspeed (IAS) below 10000 ft. Some aircraft request a higher departure speed, which is often granted. The most important reason for the speed limitation is to reduce the impact of potential bird strikes. Furthermore, this restriction helps air traffic controllers to separate planes in the dense TMA

Arriving traffic streams approach at 7000 ft. As a result, departing flight are expected to initially hold at 6000 ft. Although clearance is often given immediately to continue the climb, some flights indeed level at this altitude.

Between 21:30 and 05:30, arrivals fly the night transition approach. Aircraft remain at 7000 ft until located above the north sea where they further descent.

4-1-2 Current inefficiencies

An arbitrary nominal departure at Schiphol is shown Figure 4-1a. Although there are no extended periods of level-flight one can clearly see inefficiencies around 1500ft, 11000ft and 24500ft. To quantify this, an altitude spectrum is made similar to the one presented in Section 2-3. Using a fixed altitude interval (every 250 ft), this spectrum records the time required to climb 100ft. The result can be seen in Figure 4-1b. The red line indicates a 1000 ft/min climb rate. A major benefit of using this approach is that nominal climb rate, level-off altitudes and level-off duration can be seen in one figure.

Unfortunately, not all level-offs are performed for the same reason. Due to procedures and airspeed limitations at certain altitudes (Section 4-1-1), aircraft often accelerate by reducing the flight path angle. In order to distinguish true inefficiencies caused by air traffic control and level-offs caused by acceleration, the altitude spectrum is augmented with the ΔV_{CAS}. An example of this can be seen in Figure 4-2. Whenever a peak in the altitude spectrum coincides with a peak in ΔV_{CAS}, the inefficiency is recorded as a level-off caused by speed change. In all other cases, the inefficiency is recorded as a true level-off. Outlier-detection is used to find ΔV_{CAS} peaks.

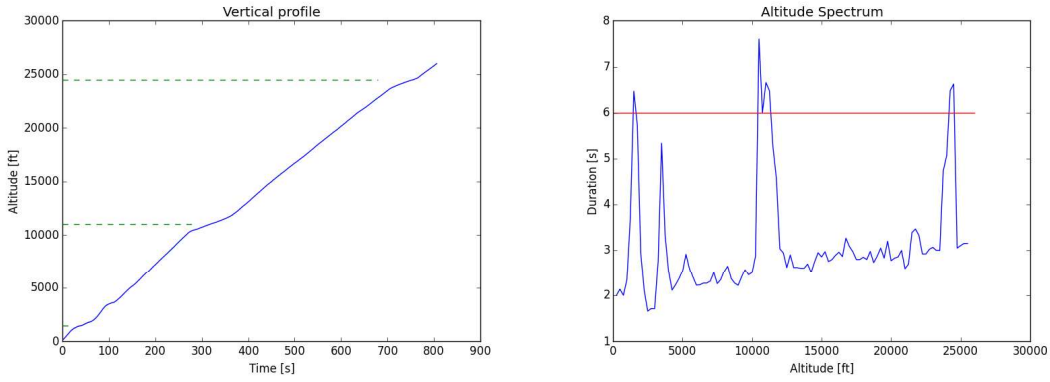

(a) Vertical climb profile **(b)** Altitude spectrum

Figure 4-1: Boeing 777 - Qatar Airways Cargo - January 1, 2017

Daily, monthly and annual variations

Applying this method to all climbing flight until July, 1 2017 gives an insight in the total number of efficiencies experienced and the daily, monthly and annual variations. Figure 4-3 shows the monthly and weekly variation. As expected, the total number of flights grows slightly going from week 1 (winter) to week 25 (summer). The occurrence of true inefficiencies however is not noticeably correlated with increase in number of flights. However, this correlation is visible when looking at the hourly variations in Figure 4-4. During the peak hours, true

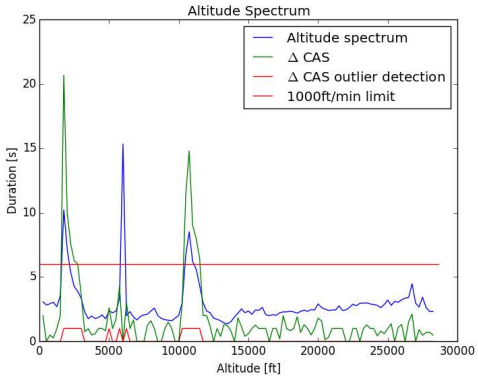

Figure 4-2: Altitude spectrum augmented with ΔV_{CAS}

level-offs occur more often than during the night and evening hours. Interestingly, the large outbound traffic density between 19:00 and 20:00 does not result in the same occurrence of true level-offs as during the morning peak. This might be a result from fact that the evening peak primarily consists of outbound traffic. This is not the case during the morning peak where arrival streams might interfere with take-off streams. One can also notice in Figure 4-5 that the inefficiencies group at certain key altitudes which correspond to the procedures described in Section 4-1-1.

Based on these finding it can be concluded that extrapolation to annual benefits in a later stage is possible when at least 1 month is analyzed. This way the hourly and daily variations are covered.

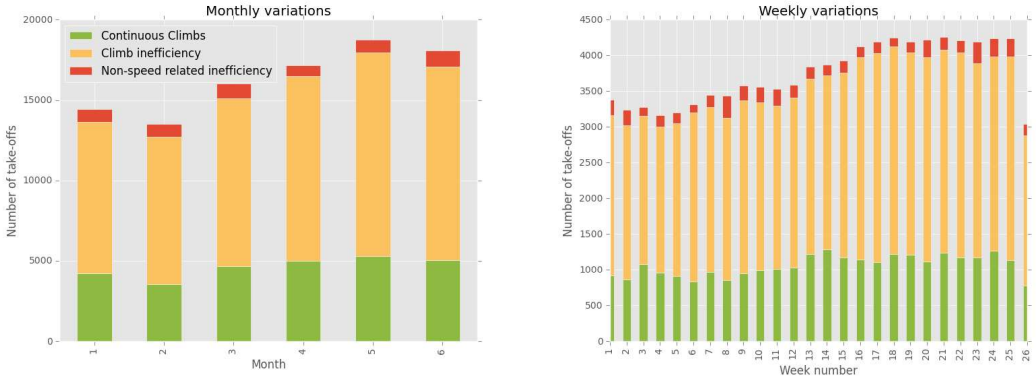

(a) Monthly variation **(b)** Weekly variation

Figure 4-3: Monthly and weekly inefficiencies of climbing flight between 1-1-2017 and 1-7-2017

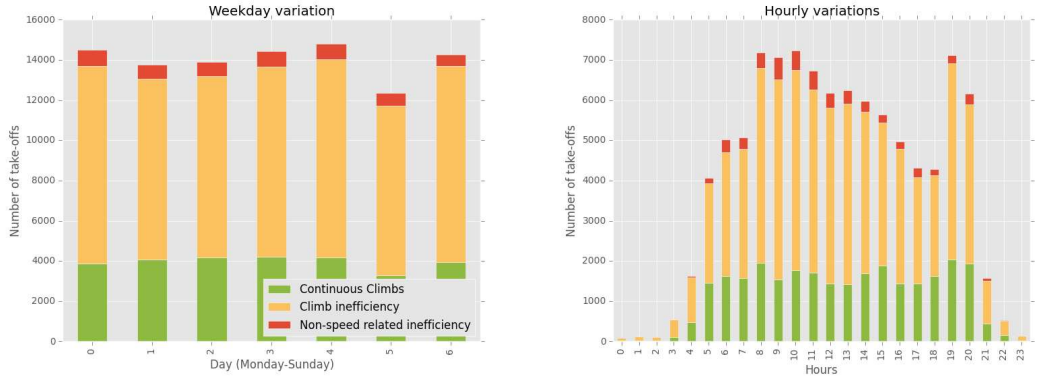

(a) Weekday variation **(b)** Hourly variation

Figure 4-4: Weekday and hourly inefficiencies of climbing flight between 1-1-2017 and 1-7-2017

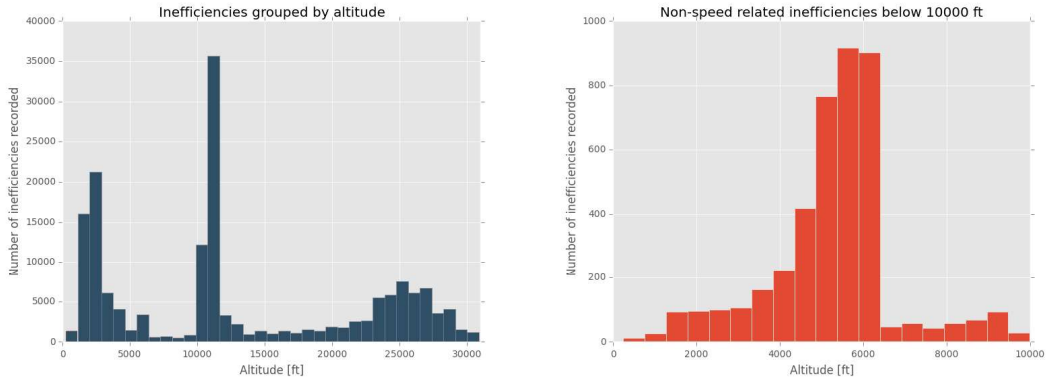

(a) Level-off distribution **(b)** True level-offs under 10000 ft

Figure 4-5: Total number of inefficiencies between 1-1-2017 and 1-7-2017 grouped by altitude

4-2 Estimating fuel consumption

The BADA performance model by Eurocontrol (n.d.) is one of the most frequently used models to estimate fuel consumption when radar track data is available. The fuel consumption is calculated by integrating fuel flow. Fuel flow is approximated by Eq. 4-1:

$$f_{nom} = C_{f1} \cdot \left(1 + \frac{V_{TAS}}{C_{f2}}\right) \cdot Thr \tag{4-1}$$

In this equation, fuel coefficient C_{f1} and C_{f1} are aircraft dependent parameters found in BADA's Aircraft Performance Operational File (OPF). True airspeed V_{TAS} has to be provided in knots. The thrust is calculated using a point-mass model in which the forces acting on the aircraft equal the change in potential en kinetic energy. This Total-Energy Model (TEM) is given by Eq. 4-2

$$(Thr - D) \cdot V_{TAS} = m \cdot g_0 \frac{dh}{dt} + m \cdot V_{TAS} \frac{dV_{TAS}}{dt} \tag{4-2}$$

With the height and speed known, the horizontal and vertical accelerations can be approximated using a discrete differentiation method. A reference mass from the OPF can be used when weight information is not present. The drag can be calculated using Eq. 4-3

$$D = \frac{C_D \cdot \rho \cdot {V_{TAS}}^2 \cdot S}{2} \tag{4-3}$$

In this equation, true airspeed V_{TAS} has to be provided in m/s and the wing reference area S in m^2. Air density ρ [kg/m^3] is dependent on the aircraft height and needs to be calculated using the ISA model. The total drag coefficient can be obtained using Eq. 4-4

$$C_D = C_{D_0} + C_{D_2} \cdot C_L^2 \tag{4-4}$$

Parasite and induced drag coefficient C_{D_0}, C_{D_2} are aircraft specific and can be found in the OPF. These values vary according to aircraft configuration and flight phase. BADA uses a 'clean' configuration for the climb phase. The lift coefficient is given by Eq. 4-5

$$C_L = \frac{2 \cdot m \cdot g_0}{\rho \cdot {V_{TAS}}^2 \cdot S \cdot \cos\theta} \tag{4-5}$$

The denominator of Eq. 4-5 contains a $\cos\theta$ term to represent the bank angle influence during turns. Since this study only considers the 2D vertical plane the bank angle is assumed to be zero which cancels the term.

4-2-1 Minimum fuel flow and maximum Climb Thrust

All engines consume a minimum amount of fuel during idle operations to maintain the thermodynamic cycle. In the BADA model, this value is given by:

$$f_{min} = C_{f3}\left(1 - \frac{h}{C_{f4}}\right) \tag{4-6}$$

In this equation, height is given h in feet, the thrust coefficient = C_{f3} in kg/min and = C_{f4} in ft. This lower limit prevents the BADA model to estimate negative fuel flow during deceleration or descent.

More relevant for climb operations is the upper thrust limit given by Eq. 4-7:

$$Thr_{max} = C_{Tc,1}\left(1 - \frac{h}{C_{Tc,2}} + C_{Tc,3} \cdot h^2\right) \tag{4-7}$$

With $C_{Tc,1}$ in N, $C_{Tc,2}$ in feet and $C_{Tc,2}$ in feet^{-2}. The maximum thrust is largely dependent on altitude and temperature. It is assumed here that there are no temperature deviations from the ISA standard atmosphere so an additional correction factor is not required. Also, Eq. 4-6 and 4-7 are only valid for jet engines. Propeller and piston engines have different equations

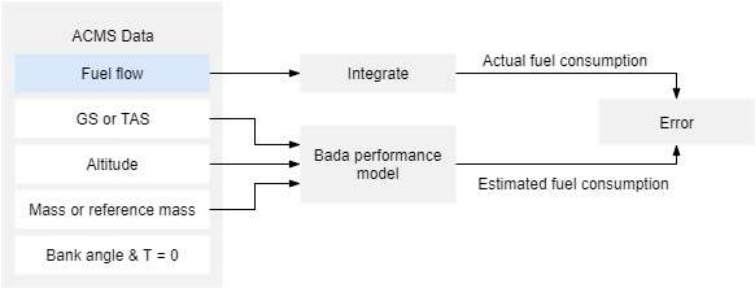

Figure 4-6: Overview of BADA validation using ACMS data

4-2-2 Assumptions

In order to scope the research and simplify some of the equations, several assumption are made. The list below provides a summary:

- BADA's total energy point mass model is used to calculate the thrust required. In this model, the bank angle is assumed to be zero. In other words, only vertical movements in the 2D plane will be considered.
- The equations and performance coefficients are valid assuming standard atmospheric conditions.
- Calculations assume zero temperature deviations compared to the ISA.
- Only aircraft with jet engines will be considered since these accounted for the majority of flight at Schiphol last year.
- Reference mass will be used for ADS-B data

4-2-3 Verification & Validation

The ACMS data provided by KLM can be used to verify the implementation of the BADA model and validate the performance. With the exact aircraft mass, altitude, airspeed and fuel flow known, the fuel estimation error of BADA can be calculated. By systematically including one assumption at the time (such as Ground Speed (GS) equals True Airspeed (TAS) or zero temperature diviations from ISA), the impact of each assumption can be calculated. A schematic overview of this process can be seen in Figure 4-6.

Although the model has been validated by Eurocontrol and independent studies (e.g. Nakamura and Kageyama (2015)), it is necessary to verify the implementation and to validate the results for atmospheric conditions, aircraft types and take-off weights at Schiphol airport. For this validation, 9285 ACMS flight records where analyzed.

Filtering airspeed and height measurements

Changes in airspeed and height are either intended, caused by turbulence or result from measurement errors. In reality, these small deviations around a mean value do not require

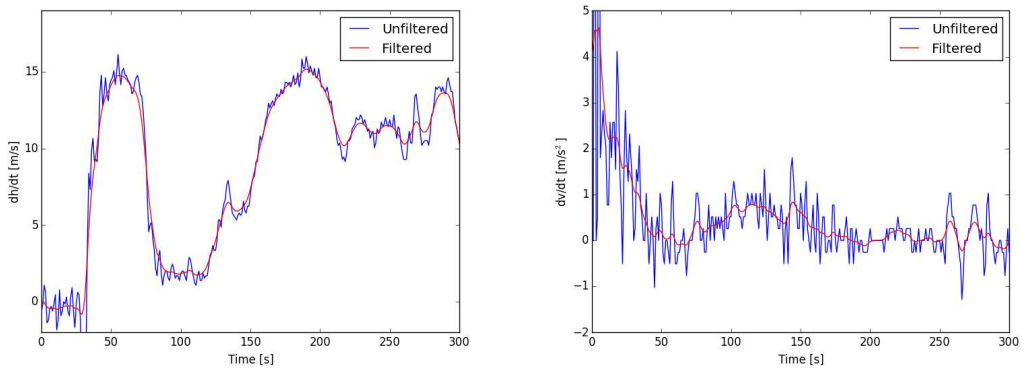

(a) Altitude derivative **(b)** True airspeed derivative

Figure 4-7: Aircraft state derivatives before and after filtering with low-pass filter

the aircraft to accelerate. The BADA model however has no knowledge of turbulence or measurement errors, so the change in height or speed is treated as acceleration caused by the engine.

The ACMS data of the KLM is measured on board and therefore records this turbulence. Since airplane dynamics are relatively slow, this can be filtered using a zero lag low-pass filter with a cut-off frequency of 0.05. The result can be seen in Figure 4-7. Optimization of the cut-off frequency with respect to the Mean Squared Error (MSE) between actual and approximated fuel burn resulted in marginal improvements.

Error between calculated and actual fuel burn

For this baseline condition, actual mass and measured TAS where inserted in the BADA model. Figure 4-8 shows the error between the estimated and actual fuel consumption recorded by the ACMS. Since this condition uses the least assumptions compared to the other conditions, this will be the baseline.

One can clearly see that the median error is less than 10 percent for all aircraft types during the climb phase. The accuracy is in line with the validation results found by Nakamura and Kageyama (2015). For most aircraft, the median error is biased to the left. This suggests that the model is slightly underestimating the fuel burn. This can be a result of ignoring bank angle or temperature deviations. A data-set with a larger variety in temperatures would rule out the last option. However, other causes such as aircraft engine degradation or measurement inaccuracy might also explain this result.

Effect of using reference mass

When using ADS-B data to estimate the fuel consumption, the aircraft mass is unknown. As a solution, BADA provides a reference mass. Figure 4-9 shows the result when using the this reference mass instead of the actual mass.

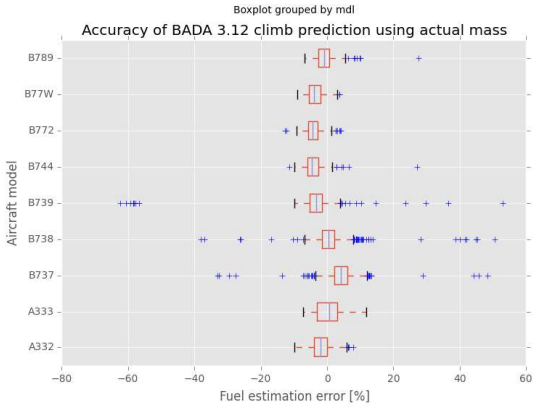

Figure 4-8: Error between actual and estimated fuel consumption (Baseline)

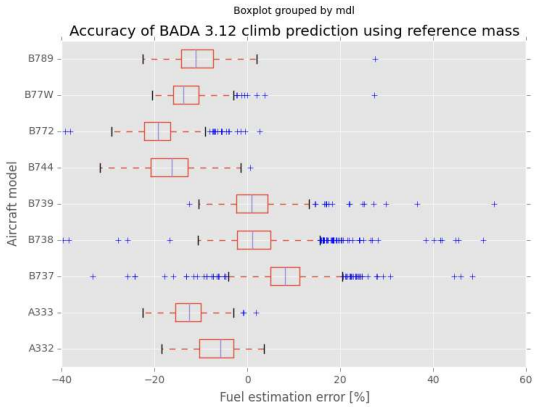

Figure 4-9: Error between actual and estimated fuel consumption (reference mass)

Comparing Figure 4-9 and 4-8 it can be seen that the error significantly increases when using the actual take-off mass. Especially for the larger long-range aircraft. The idea rises that the short-haul medium sized aircraft generally depart with a mass close to the reference. On the other hand, it appears that large long-range aircraft are often loaded closer to Maximum Take-off Weight (MTOW)

In order to investigate this statement, the historic distribution of actual mass during take-off is shown in Figure 4-10. The green, orange and red line indicate the minimum, reference and maximum take-off mass respectively.

According to Figure 4-10, two aircraft take-off with a mass higher than the MTOW. This can be explained by the fact that BADA makes no distinction between for example an Airbus A330-300 and the newer A330-303 which is owned by KLM. This newer version has a significantly upgraded MTOW.

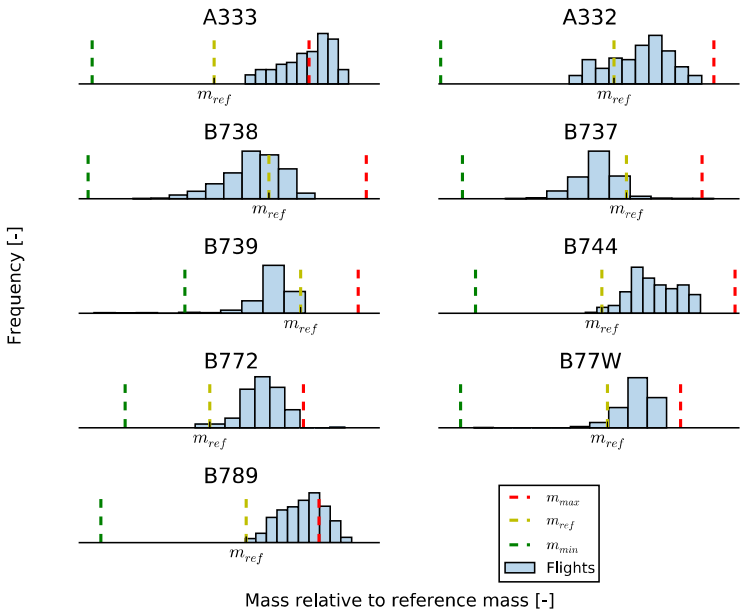

Figure 4-10: Distribution of actual take-off mass with respect to BADA reference mass

Effect of assuming zero ISA temperature deviation

Assuming no temperature deviations from ISA result in slightly under or over-estimated engine performance. Figure 4-11 shows the baseline fuel estimation error with respect to the measured ΔT temperature deviation from the standard $T_0 = 288.15K$ at MSE. The error appears to increase in the direction of increasing negative ΔT. Drawing conclusions based on this result is not entirely valid since the number of datapoints is not equally distributed over the entire temperature range.

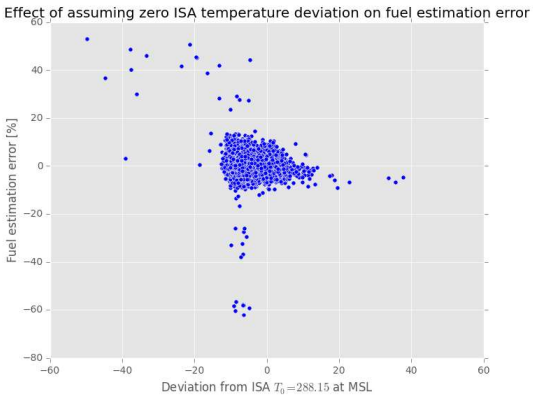

Figure 4-11: Effect of outside temperature on estimation error

Effect of assuming TAS equals GS

Without accurate wind-speed and wind-direction data, it is not possible to calculate TAS from GS when using ADS-B radar data. Figure 4-12 shows the fuel estimation error when GS is used instead of TAS. Comparing this to the baseline condition in Figure 4-8, one can see that this assumption has little influence on the error.

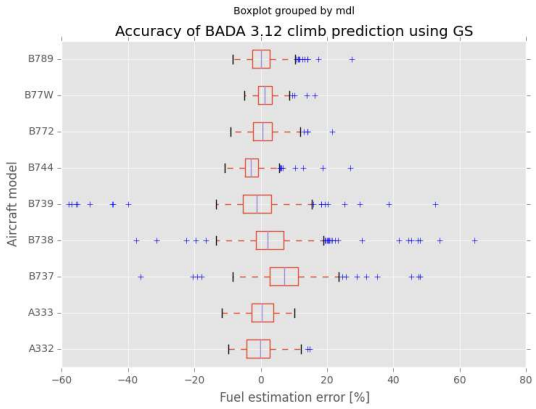

Figure 4-12: Error between actual and estimated fuel consumption (ground speed)

To investigate if there is a correlation between wind speed and fuel estimation error during climb, average wind-speed and wind-direction are plotted against this relative error (Figure 4-13). It can be seen that the majority of take-offs is performed with wind speeds under 40 kts. Above this speed, the error often increases above ±15%.

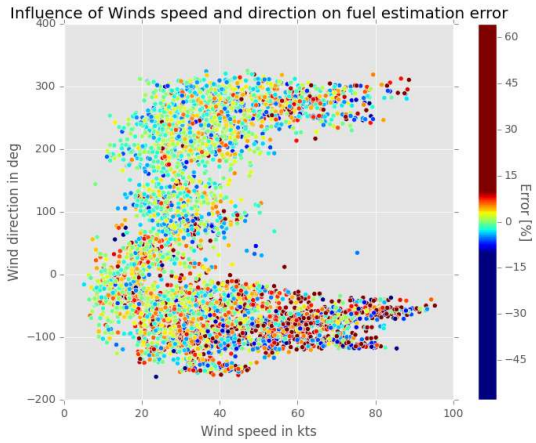

Figure 4-13: Wind-speed and wind-direction versus estimation error

It can be concluded that the BADA model is correctly implemented. However, during the climb phase the weight of aircraft can deviate significantly from the reference mass. This can have a large influence on the estimation of fuel consumed.

4-3 Theory on fuel optimized climb trajectories

Until now, most studies assessed the benefits of CCO by removing the level-flight segments. The question remains if this is the most fuel optimal ascend, and whether a fully fuel-optimized path is realistic in current-day operations. Nevertheless, comparing the current situation with a theoretical optimum gives insight in how much current operations deviate from this.

The general principle of a fuel-economic climb is to ascend to lower air density as quickly as possible using the aircrafts most efficient airspeed. During climb, the excess between power available and power required can be used to either accelerate along the flight path or gain altitude. The ideal allocation of power between these two components is continuously changing in time. The calculation of such an optimized path can be done in several ways depending on the assumptions used. Because of the large dependencies between airspeed, air density, thrust, drag and fuel consumption. This optimization problem quickly grows in complexity when removing assumptions.

This section describes several methods to find a trade-off between computational effort and realism.

4-3-1 Quasi-steady symmetric flight

One way to analytically approximate the minimum-fuel problem is to assume the following:

- No accelerations: straight flight, constant γ
- Maximum Thrust aligned with the flightpath (Figure 4-14).
- Thrust independent of airspeed,
- Constant mass during climb
- No wind
- Standard Atmosphere
- Jet or turbofan engine

According to Ruijgrok (2007), it is commonly assumed that thrust for jet engines is independent of airspeed. Figure 4-15 shows the almost straight relation between thrust and airspeed. The altitude however has a large influence on thrust since it is commonly assumed that thrust decreases proportional to air density. The weight of the fuel burned during a certain amount of time can be approximated by:

$$W_f = \int_{t_0}^{t_1} Thr(\rho) \cdot c_T \quad dt \tag{4-8}$$

Since engine thrust coefficient c_T is assumed independent of time, and Thr linearly decaying with altitude, the only way to minimize the total fuel burned during climb under these assumptions is to minimize the time to reach a certain altitude:

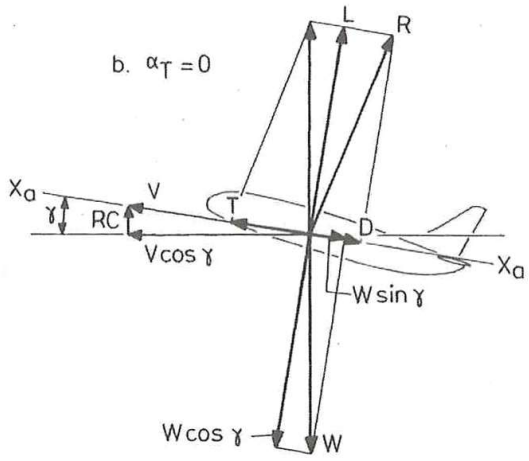

Figure 4-14: Sketch of airplane in steady symmetric flight (Ruijgrok, 2007)

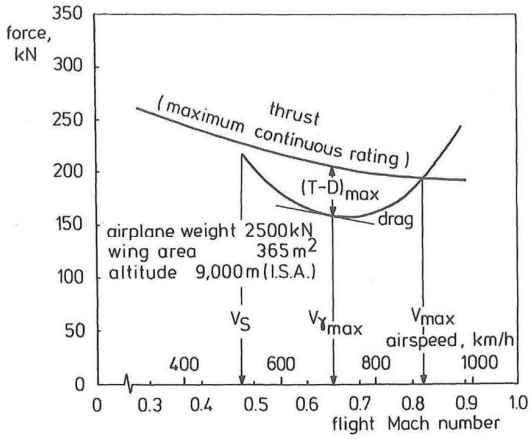

Figure 4-15: Relation between Thrust, drag and Mach number for jet engines (Ruijgrok, 2007)

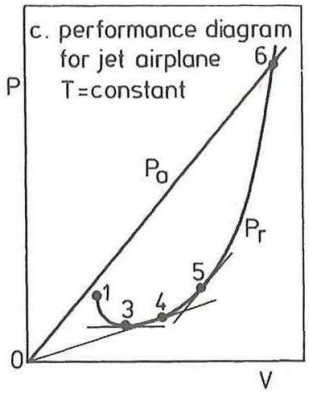

Figure 4-16: Power available and power required versus airspeed (Ruijgrok, 2007)

$$\frac{dh}{dt} = RC = V \cdot \sin\gamma \tag{4-9}$$

$$t_{min} = \int_{h_0}^{h_1} \frac{1}{RC_{max}} dh \tag{4-10}$$

In order to minimize the time, the rate of climb needs to be maximized. This can be achieved by flying the airspeed at which the difference between power available and power required is the largest.

$$RC_{max} = \frac{(P_a - P_r)_{max}}{W} = \frac{(TV - DV)_{max}}{W} \tag{4-11}$$

Under the assumption that thrust is constant over airspeed, the power available ($P_a = T \cdot V$) varies linearly with airspeed. At point 5 in Figure 4-16, the tangents of both power curves are parallel. This location corresponds to the airspeed at which excess power is largest, hence at which the rate of climb is maximized. In order to find the airspeed which corresponds to this point, the derivative with respect to airspeed should be calculated for both Pa and Pr in Eqn. 4-12.

$$\frac{d(Pa)}{dV} = \frac{d(Pr)}{dV} \tag{4-12}$$

As mentioned earlier, the thrust (and drag) decreases with altitude. The optimal airspeed to fly the maximum rate of climb therefore slightly increases over altitude. Figure 4-17 shows a sketch of the development of TAS versus altitude at maximum RC. When airline pilots would continuously climb at RC_{max}, the equivalent airspeed would slowly decrease. Since current procedures involve climbing at constant Calibrated Airspeed (CAS), this would impose an operational challenge and requires adaption of the current autopilot systems.

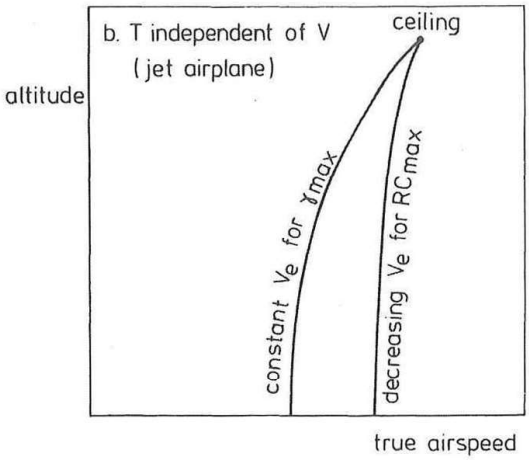

Figure 4-17: Sketch of optimal TAS for maximum RC versus altitude (Ruijgrok, 2007)

4-3-2 Unsteady quasi-rectilinear climb

When climbing according to the maximum rate of climb speed found in the previous section, the true airspeed increases with height. This implies that part of the excess power available will be used to accelerate along the flight path. In other words, the climb becomes unsteady. A method proposed by Ruijgrok (2007) is to calculate the fuel optimal climb using an energy-state approximation summing potential and kinetic energy:

$$E = WH + \frac{W}{2g_0}V^2 \tag{4-13}$$

Dividing by weight to obtain specific energy and differentiating with respect to obtain:

$$\frac{dH_e}{dt} = \frac{dH}{dt} + \frac{V}{g_0}\frac{dV}{dt} \tag{4-14}$$

Substituting Eq. 4-9:

$$\frac{dH_e}{dt} = V\left(\sin\gamma + \frac{1}{g_0}\frac{dV}{dt}\right) \tag{4-15}$$

Introducing the equation of motion parallel with the flight direction in figure 4-14:

$$\frac{W}{g_0}\frac{dV}{dt} = T - D - Wsin\gamma \tag{4-16}$$

Dividing by aircraft weight W and rearranging:

$$\frac{T-D}{W} = sin\gamma + \frac{1}{g_0}\frac{dV}{dt} \tag{4-17}$$

Substituting Eq. 4-17 in Eq. 4-15 gives:

$$\frac{dH_e}{dt} = \frac{V(T-D)}{W} = RC_s \tag{4-18}$$

In other words, the energy-height time derivative equals the RC of a quasi-steady flying aircraft. Rearranging and integration gives:

$$t = \int_{H_{e_1}}^{H_{e_2}} \frac{dH_e}{RC_s} \tag{4-19}$$

Using all but the first assumptions stated in 4-3-1, a fuel optimal climb equals a minimum-time climb. Therefore, the steady-state RC_s needs to be maximized at each energy height. This can be done in a similar fashion a the method presented in the previous section.

4-3-3 Approximating realistic optimal climb operations

The methods described in the sections above are neglecting parameters of the climb that have a large influence on the fuel consumption and trajectory in order to simplify the problem. Parameters such as weather, temperature, changing mass, true engine performance and CI all affect the optimal airspeed.

In light of this, two recent studies have investigated a fuel-optimized climb. Rosenow, Forster and Fricke 2016 Rosenow and Stanley (2016) state that an optimized climb can be achieved by reducing the number of thrust changes and eliminating the level-offs. This prevents excessive acceleration forces which in turn minimizes the fuel consumption. In other words, the true airspeed of the aircraft at the end of climb should equal the desired cruise speed. The main challenge is the influence of real atmospheric conditions. Due to the constant changes in airspeed and acceleration, the optimization problem becomes unstable. Rosenow developed a 3D aircraft performance model COALA (partially based on BADA3 and 4 coefficients) and varied the true airspeed to investigate various climb angles and climb speeds. Analyzing 4 commercial aircraft types, it was found that climbing at a maximum climb rate resulted in an almost fuel-optimal climb. It has to be noted that, since only 4 aircraft types and one atmospheric condition has been used, the results can not be generalized.

The second result in 2016 came from a study by Hartjes and Visser (2016). This study was done for Schiphol Airport and investigated 3D flightpath optimization using a genetic algorithm. One existing SID was optimized on noise and fuel while still satisfying regulations and constraints of the airspace. Four resulting cases where found: two extreme cases fully optimized on either noise or fuel consumption and two moderate cases combining both criteria. Interestingly, the two moderate cases turned out to be non-continuous climbs. No further profile information was given for fuel-optimized extreme case.

Real-life operations are flown using a constant CAS (or IAS) climb speed. Until 10000 ft, this CAS speed is limited to 250 kts. Beyond this point, a constant CAS is maintained until the cruise Mach number is reached. From this point on, aircraft proceed climbing with constant Mach number. This implies that the TAS decreases from that point on. If you would continue climbing at constant CAS, the aircraft will approach the speed of sound. The optimal CAS and Mach settings are determined by an optimization routine incorporating weather, mass and CI. Since airlines do not publish the CI, it is hard to estimate the effect of this parameter on the CAS flown. However, there exists a constant CAS speed (and Mach setting) which corresponds to a Cost index of 0. In other words, the most fuel optimized climb. It has to be noted that this climb still deviates from a theoretically optimal climb since this would require the CAS to be variable with altitude.

4-3-4 Analysis

Several papers identified that climbing close to maximum climb rate will result in a fuel optimized climb. Under the assumptions stated in section 4-3-1, it was also shown that flying at maximum rate of climb turns out to be the most fuel optimal method. This climb corresponds to a Cost-Index of 0. In everyday operations, this Cost-Index value might not be realistic since the cost of time has to be taken into account. Nevertheless, comparing the current situation with a theoretical optimum gives insight in how much current operations deviate from this.

With these results, the choice has been made to create a trajectory model which approaches maximum climb rate. This will be done by assuming a constant (reduced) thrust setting until cruise altitude. The aircraft will also fly at a constant CAS speed until the cruise mach number is achieved. This way, the number of thrust and speed changes will be reduced to a minimum. The unknown variable is the CAS setting.

4-4 Trajectory Model

As discussed in previous sections, airlines climb using constant CAS and Mach settings. The choice has been made to create an trajectory model according to this procedure. As explained in section 4-3. Climbing at a constant CAS setting requires the aircraft to assign a part of the excess energy to an increase in TAS instead of altitude. To determine this ratio, BADA uses the Energy Share Factor (ESF), which will form the foundation of the trajectory model.

4-4-1 Basic Equations

A sketch of a single time step is given in Figure 4-18. Starting at t_i, the next ($\Delta t = 1s$) time step t_{i+1} can be calculated using:

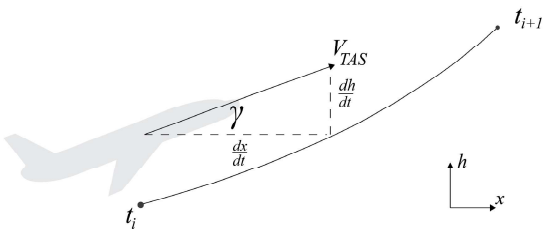

Figure 4-18: Sketch of a time-step in the trajectory model

$$\begin{aligned} h(t_{i+1}) &= h(t_i) + \frac{dh}{dt} \\ V_{TAS}(t_{i+1}) &= V_{TAS}(t_i) + \frac{dV_{TAS}}{dt} \\ x(t_{i+1}) &= x(t_i) + \frac{dx}{dt} \end{aligned}$$

With starting conditions known, these equations can be solved by isolating $\frac{dh}{dt}$, $\frac{dv}{dt}$, $\frac{dx}{dt}$ from the TEM in Eqn. 4-2 results in:

$$\frac{dh}{dt} = \frac{(Thr - D)V_{TAS}}{m \cdot g_0} f\{M\} \tag{4-20}$$

$$\frac{dv}{dt} = \frac{dv}{dh}\frac{dh}{dt} = \left[\left(\frac{1}{f\{M\}} - 1\right)\frac{g_0}{V_{TAS}}\right]\frac{dh}{dt} \tag{4-21}$$

$$\gamma = \sin^{-1}\left(\frac{\frac{dh}{dt}}{V_{TAS}}\right) \tag{4-22}$$

$$\frac{dx}{dt} = V_{TAS}\cos\gamma \tag{4-23}$$

In which the ESF is given by:

$$f\{M\} = \frac{1}{1 + \frac{V_{TAS}}{g_0}\frac{dV_{TAS}}{dh}} \tag{4-24}$$

To solve these equations the Thrust, Drag and $f\{M\}$ need to be calculated at each time-step. Throughout the entire climb, the thrust setting will be held constant at a reduced climb power setting. This is common practice to reduce engine wear. The drag can be calculated using the equations in Section 4-2. According to BADA, reduced thrust can be approximated by multiplying the left-hand side of Eqn. 4-2 with:

$$C_{reduced} = 1 - 0.15\frac{m_{max} - m_{act}}{m_{max} - m_{min}} \tag{4-25}$$

4-4-2 Energy Share Factor

Instead of calculating the $f\{M\}$ using Eqn.4-24, the ratio of speed change over altitude change can be calculated using Eqns. 4-26 to 4-29 (Eurocontrol, n.d.). These equations calculate the acceleration required to maintain a constant CAS or Mach at a given altitude. Below the tropopauze, climbing at constant CAS, the ESF can be calculated using:

$$f\{M\} = \left[1 + \frac{\kappa R \beta}{2g_0} M^2 + \left(1 + \frac{\kappa - 1}{2} M^2\right)^{\frac{-1}{\kappa-1}} \left(\left(1 + \frac{\kappa - 1}{2} M^2\right)^{\frac{\kappa}{\kappa-1}} - 1\right)\right]^{-1} \tag{4-26}$$

Above the tropopause, the equation reduces to:

$$f\{M\} = \left[\left(1 + \frac{\kappa - 1}{2} M^2\right)^{\frac{-1}{\kappa-1}} \left(\left(1 + \frac{\kappa - 1}{2} M^2\right)^{\frac{\kappa}{\kappa-1}} - 1\right)\right]^{-1} \tag{4-27}$$

When the Mach/CAS transition takes place below the tropopause, the aircraft will continue climbing at constant Mach number which reduces the ESF further to:

$$f\{M\} = \left[1 + \frac{\kappa - 1}{2} M^2\right]^{-1} \tag{4-28}$$

Flying at constant Mach above the tropopause requires no deceleration or acceleration. In other words, all the excess power can be used to climb:

$$f\{M\} = 1 \tag{4-29}$$

4-4-3 Algorithm Flowchart

The general principle of the trajectory model is to start at a given altitude, speed and distance: h_0, v_0 & x_0. These values are used to calculate the atmoshperic properties and Mach number. In turn, this determines if boundary, height or speed conditions are met and which type of Equation is valid to calculate the ESF. With the ESF known, the rate of speed and climb is used to calculate the next time step. The process continues until the cruise height is reached. From this point on, all excess energy will be used to accelerate to the pre-determined speed and distance. The latter is necessary to ensure a fair comparison between the different profiles. An aircraft with a higher constant CAS/Mach setting will have traveled a longer distance when reaching cruise altitude than one climbing at a lower CAS. A flowchart of the algorithm is given in Figure 4-19. In Appendix C, several resulting trajectories are shown for a single flight optimized from 3000 ft and 10000 ft (Figure C-1, C-1).

4-4-4 Flight envelope

After each time-step, the model checks if the current airspeed is still within the aircraft flight envelope. Minimum speed, maximum operating CAS and maximum operational Mach number are compared with the values specified in BADA's OPF file.

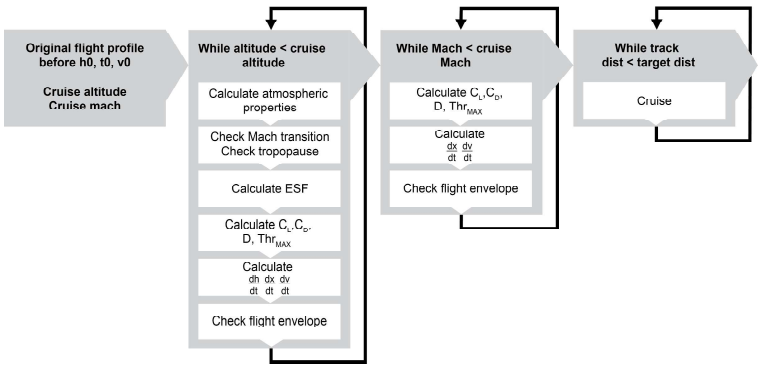

Figure 4-19: Flowchart of the trajectory model

The maximum speeds are the most limiting factor in trajectory design. The minimum speed is (in the specific simulations for this thesis) never reached due to the range of CAS values considered. Therefore, the low-speed buffeting limit is neglected and only minimum speed is checked for comprehensiveness.

4-4-5 Mass Sensitivity

In Figure 4-20, the climb of an Airbus A330-300 is simulated for 4 different conditions. The first two profiles on the left correspond to a take-off weight of $180 \cdot 10^3$ kg. The two profiles on the right correspond to a weight of $210 \cdot 10^3$ tonnes. Both conditions are flown with an optimized and non-optimized speed. When estimating the fuel consumption of these profiles using BADA, it was found that approximately 30 kg can be saved on the low weight configuration and 50 kg on the heavy configuration.

However, comparing two profiles with a different weight would result in roughly 500 kg difference. A similar problem occurs when using ADS-B data. Since aircraft mass is unknown, a new profile would be calculated using reference mass. If the original flight would have been flown with a deviating mass, the resulting historical profile would have been completely different. The uncertainty in weight causes a difference in fuel consumption which is an order of magnitude larger compared to potential fuel savings gained by optimizing the climb. Based on this result it can be concluded that reference mass is insufficient for analysis of the climb phase.

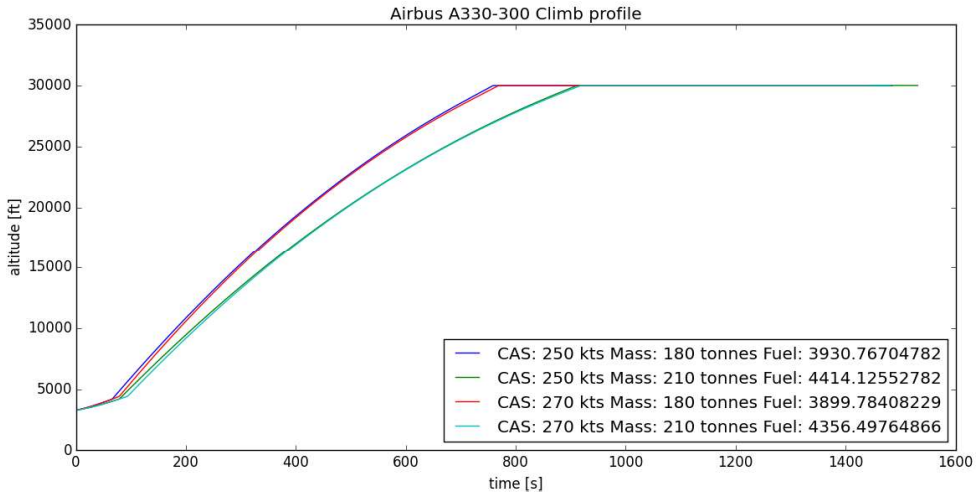

Figure 4-20: Effect of mass uncertainty on climb profiles

4-5 Initial Results

The first optimization run has been performed on 9285 ACMS records. During these simulations, the first 3000 ft from the original historic flight have been copied into the trajectory model. From this point on, the profile was optimized for constant CAS. The results can be seen in Figure 4-21 - 4-22.

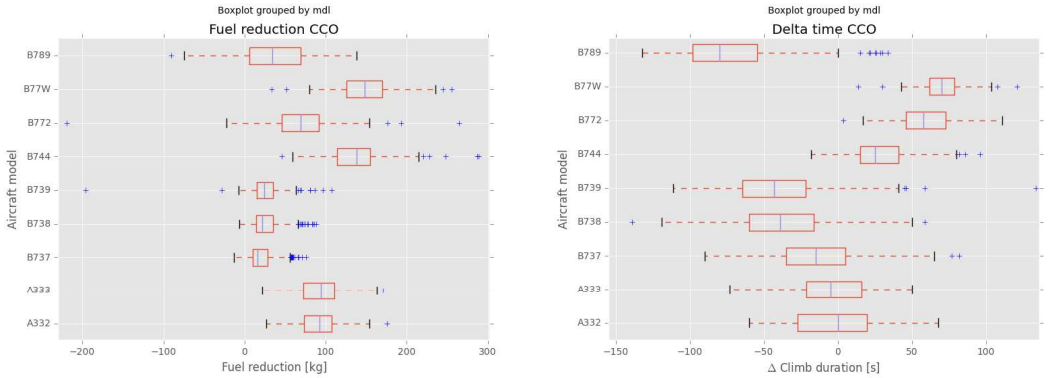

(a) Fuel benefits [kg] **(b)** Time benefits [s]

Figure 4-21: Results (fuel and time) of first optimization run starting at 3000 ft

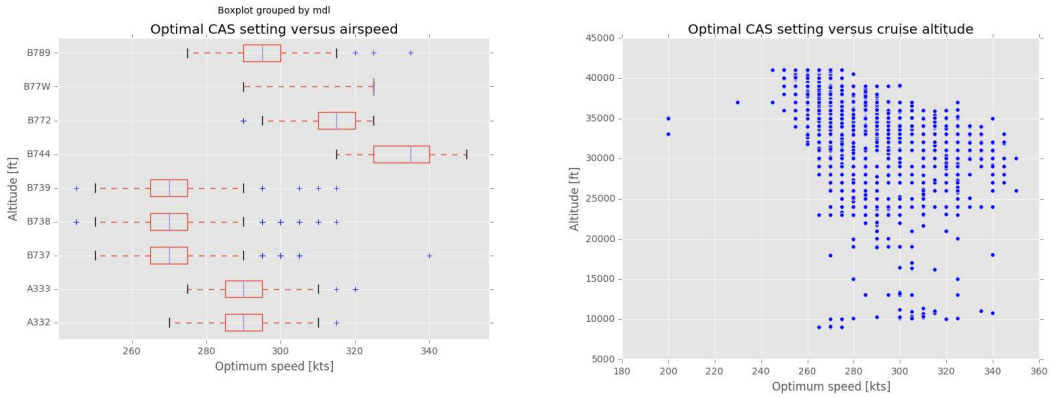

(a) Optimal constant CAS [kts] **(b)** Optimal cas versus cruise altitude

Figure 4-22: Results (speed) of first optimization run starting at 3000 ft

Appendix A

Data sources and variables

Table A-1: Availability of variables and parameters from ACMS and ADS-B data sources

ACMS	**ADS-B**
Time and Date	Unix timestamp
Aircraft Registration	ICAO aircraft address
Aircraft Type	Latitude
Flight Number	Longitude
Departure Station	Altitude
Runway	Ground speed
Pitch	Heading
Flaps	Rate of Climb
FMA settings (VNAV)	Callsign
Latitude	
Longitude	
Standard Altitude	
Radio Altitude	
Ground speed	
True Airspeed	
Indicated Airspeed	
Mach	
Inertial Vertical Speed	
Outside Static Air Temperature	
Total Air Temperature	
Wind speed	
Wind direction	
Total Fuel Quantity	
Gross Weight	
A/P #1 Engaged	
A/P #2 Engaged	
Fuel Flow ENG #1	
Fuel Flow ENG #2	
N1 ENG #1	
N1 ENG #2	

Appendix B

Schiphol SID Chart

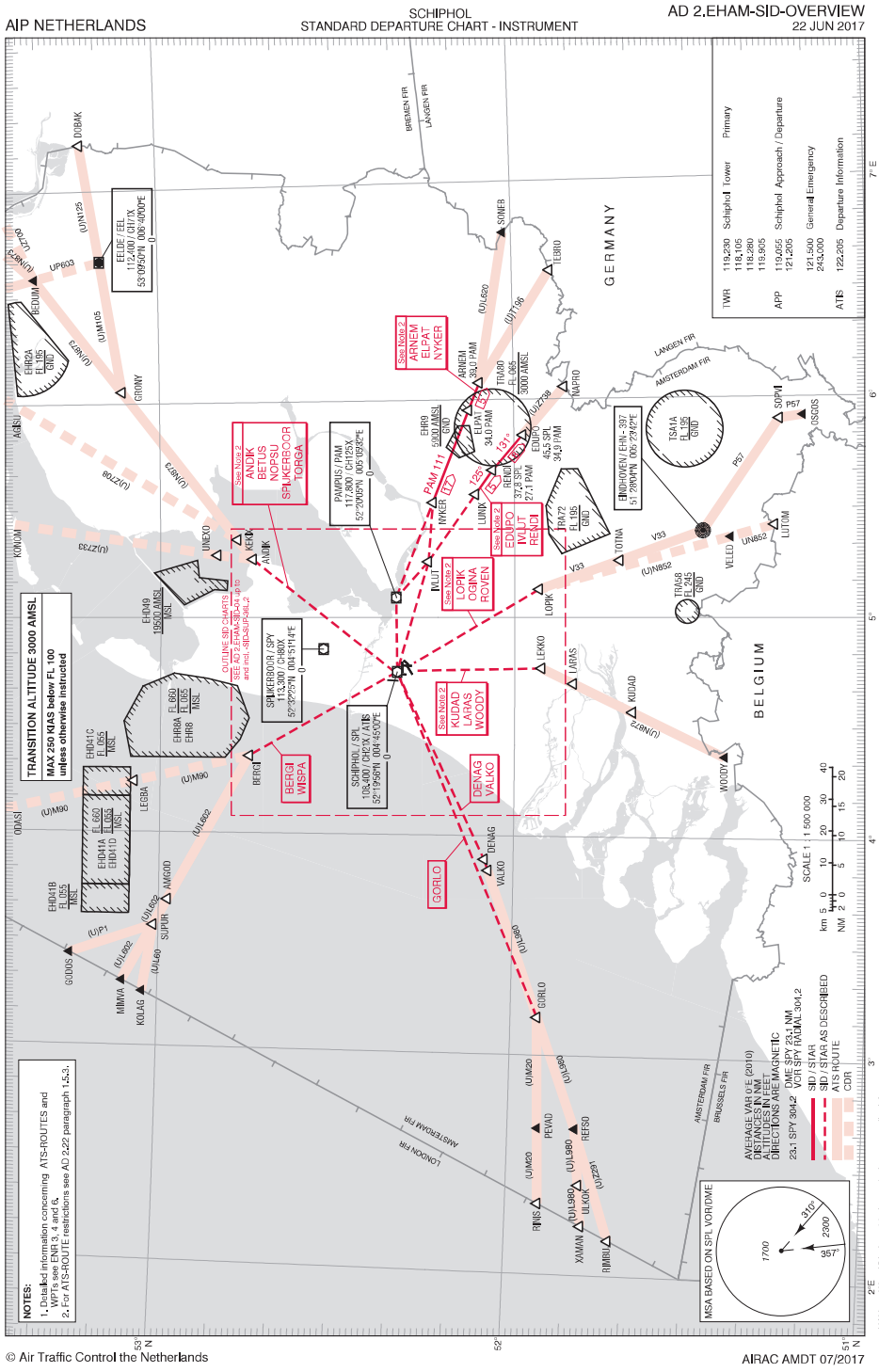

Figure B-1: Overview of SID routes departing Schiphol (AIS-Netherlands)

Appendix C

Trajectory model

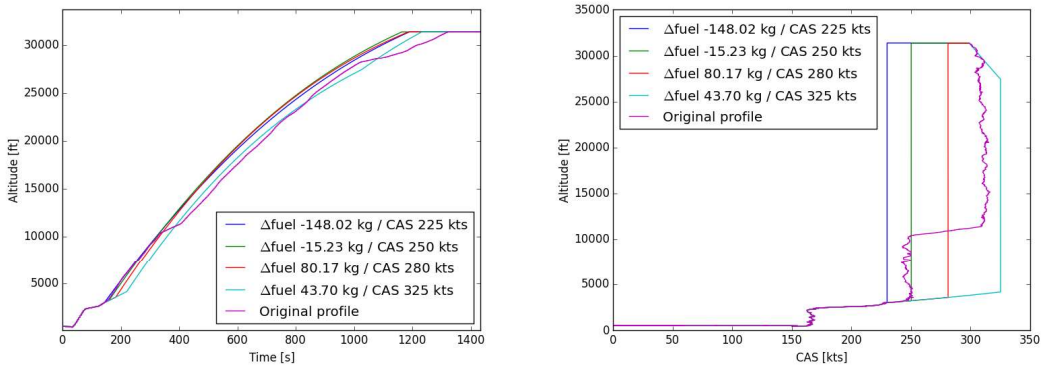

(a) Altitude vs. time **(b)** Altitude vs. airspeed

Figure C-1: New climb trajectories (optimized from 3000ft) versus historic flight Airbus A330 PH-AKA

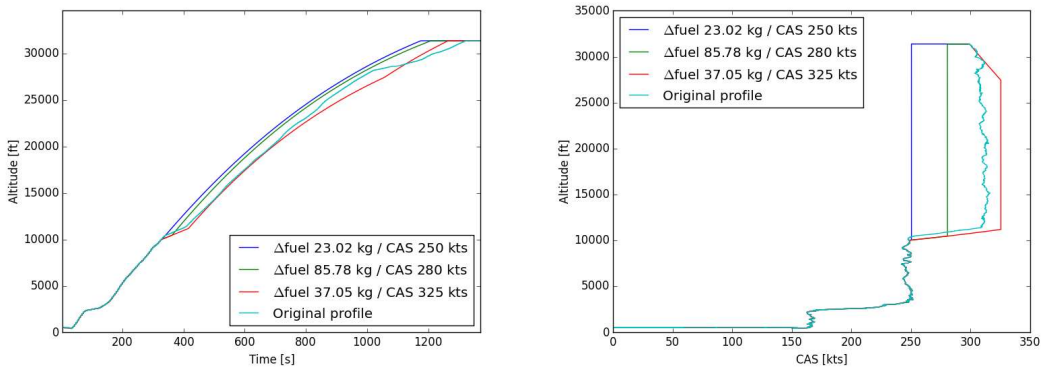

(a) Altitude vs. time **(b)** Altitude vs. airspeed

Figure C-2: New climb trajectories (optimized from 10,000ft) versus historic flight Airbus A330 PH-AKA

Appendix D

Gantt Chart

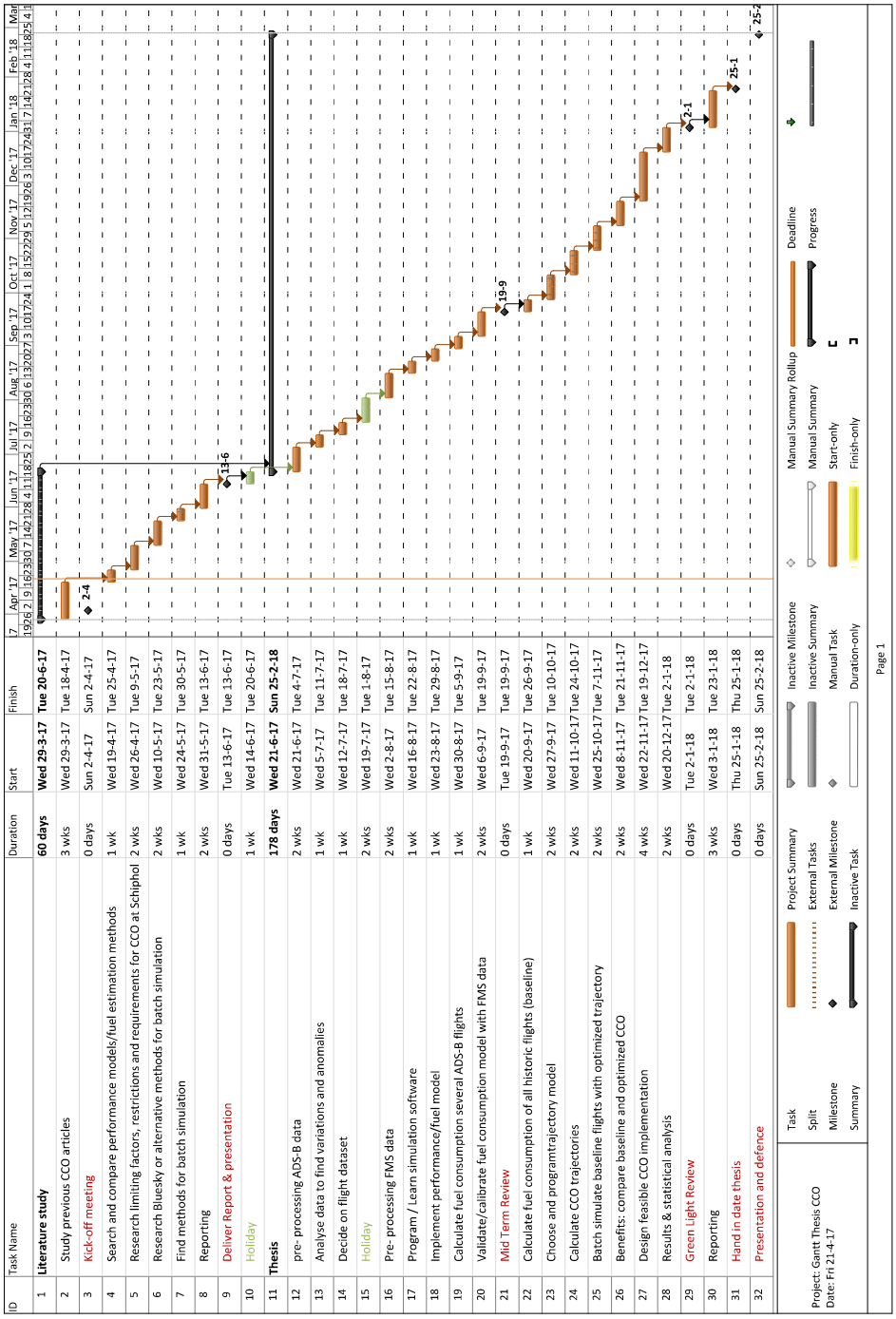

Figure D-1: Project planning visualized using a Gantt Chart

Bibliography

Dalmau, R., & Prats, X. (2015). Fuel and time savings by flying continuous cruise climbs. estimating the benefit pools for maximum range operations. *Transportation Research Part D: Transport and Environment*, *35*, 62-71. (cited By 4) doi: 10.1016/j.trd.2014.11.019

Eurocontrol. (n.d.). *Base of aircraft data v3.12.* Retrieved 2017-09-10, from `https://www.eurocontrol.int/services/bada`

Federal Aviation Administration, M. (2015). 2014 optimization of airspace and procedures for metroplex (oapm) houston metroplex post implementation analysis. *AIAA's 3rd Annual Aviation Technology, Integration, and Operations (ATIO) Forum.*

Hartjes, S., & Visser, H. (2016). Efficient trajectory parameterization for environmental optimization of departure flight paths using a genetic algorithm. *Proceedings of the Institution of Mechanical Engineers, Part G: Journal of Aerospace Engineering*, *231*(6), 1115–1123. doi: 10.1177/0954410016648980

ICAO. (2013). *"continuous climb operation (cco) manual".*

Jung, Y., & Isaacson, D. (2003). Development of conflict-free, unrestricted climbs for a terminal area departure tool.. (cited By 7)

McConnachie, D., Bonnefoy, P., & Belle, A. (2015). Investigating benefits from continuous climb operating concepts in the national airspace system: Data and simulation analysis of operational and environmental benefits and impacts.. (cited By 3)

Melby, P., & Mayer, R. (2008). Benefit potential of continuous climb and descent operations.. (cited By 0)

Miller, M., Graham, M., & Aldous, J. (2011). Efficient climb and descent benefit pool.. (cited By 0) doi: 10.1109/DASC.2011.6096003

Nakamura, Y., & Kageyama, K. (2015). Study on validation and application of fuel-burn estimation.. (cited By 0)

Roach, K., & Robinson III, J. (2010). A terminal area analysis of continuous ascent departure fuel use at dallas/fort worth international airport. In (Vol. 3). (cited By 2) doi: 10.2514/6.2010-9379

Rosenow, J., & Stanley, F. (2016). Continuous Climb Operations with Minimum Fuel Burn. (November).

Ruijgrok, G. (2007). *Elements of airplane performance* (2nd ed.). Delft: VSSD.

Schiphol traffic review 2016. (n.d.). https://www.schiphol.nl/en/schiphol-group/page/traffic-review. (Accessed: 2017-07-03)

Vempati, L. (2015). Observed impact of traffic and weather on continuous descent and continuous climb operations. In (p. 1C51-1C58). (cited By 0) doi: 10.1109/DASC.2015.7311343